Co-chaperone CHIP Associates with Expanded Polyglutamine Protein and Promotes Their Degradation by Proteasomes*

Nihar Ranjan Jana‡§¶, Priyanka Dikshit‡¶, Anand Goswami‡, Svetlana Kotliarova∥, Shigeo Murata**, Keiji Tanaka**, and Nobuyuki Nukina∥‡‡

From the ‡Cellular and Molecular Neuroscience Laboratory, National Brain Research Centre, Manesar, Gurgaon 122-050, India, the ∥Laboratory for Structural Neuropathology, RIKEN Brain Science Institute, 2-1 Hirosawa, Wako-shi, Saitama 351-0198, Japan, and the **Department of Molecular Oncology, Tokyo Metropoliton Institute of Medical Science, Bankyo-ku, Tokyo 113-8613, Japan

A major hallmark of the polyglutamine diseases is the formation of neuronal intranuclear inclusions of the disease proteins that are ubiquitinated and often associated with various chaperones and proteasome components. But, how the polyglutamine proteins are ubiquitinated and degraded by the proteasomes are not known. Here, we demonstrate that CHIP (C terminus of Hsp70-interacting protein) co-immunoprecipitates with the polyglutamine-expanded huntingtin or ataxin-3 and associates with their aggregates. Transient overexpression of CHIP increases the ubiquitination and the rate of degradation of polyglutamine-expanded huntingtin or ataxin-3. Finally, we show that overexpression of CHIP suppresses the aggregation and cell death mediated by expanded polyglutamine proteins and the suppressive effect is more prominent when CHIP is overexpressed along with Hsc70.

The pathological expansion of unstable trinucleotide repeats has been found to cause 15 neurological diseases, 9 of which are neurodegenerative diseases (also referred to as polyglutamine diseases) resulting from the expansion of CAG repeats within the coding region of the responsible genes. Those nine include Huntington's disease (HD),[1] dentatorubral pallidoluysian atrophy, X-linked spinal bulbar muscular atrophy (SBMA), and several spinocerebellar ataxias (SCA1, SCA2, SCA3, SCA6, SCA7, and SCA17). All nine disorders are progressive, dominantly inherited (except spinal bulbar muscular atrophy), typically begin in midlife, and result in severe neuronal dysfunction and neuronal cell death. Increasing length of glutamine repeats in the affected individual strongly correlates with earlier age of onset and disease severity (1).

Evidence suggests a toxic gain-of-function effect of the poly-glutamine expansion on the protein, and this novel neurotoxic property most likely involves an increased propensity for the disease protein to aggregate (2). In human disease tissue, transgenic animal models, and transfected cells expanded polyglutamine proteins have been shown to undergo intracellular aggregation, in most cases forming neuronal intranuclear inclusions (3). However, the discovery of ubiquitinated aggregates or the neuronal intranuclear inclusions and the association of various chaperones and proteasome components with the aggregates suggest that the cells recognize the aggregated disease protein as abnormal and may represent an appropriate cellular response to refold or degrade aggregated mutant protein (4–9). Consistent with this idea, it has been experimentally demonstrated that overexpression of selective chaperones in the mammalian cell culture suppresses the aggregate formation and cell death (4, 6, 7, 9) and that the proteasome system is indeed involved in the degradation of polyglutamine proteins (5, 10, 11). However, very little is known about the delivery of the expanded-polyglutamine proteins to the ubiquitin proteasome pathway (UPP) for degradation.

In the present investigation, we studied the detail mechanism of ubiquitination of the expanded polyglutamine proteins using polyglutamine-expanded truncated N-terminal huntingtin (tNhtt) as well as truncated ataxin-3 as models. We found that CHIP, an ubiquitin ligase, associates with the expanded polyglutamine proteins and is responsible for their ubiquitination and degradation by proteasomes.

EXPERIMENTAL PROCEDURES

Materials—Lactacystin, 3-(4,5-dimethylthiazol-2-yl)-2,5-diphenyltetrazolium bromide (MTT), dbcAMP, and all cell culture reagents were obtained from Sigma. Lipofectamine 2000, Zeocin, G418, ponasterone A, and mouse monoclonal anti-v5 were purchased from Invitrogen. Rabbit polyclonal anti-ubiquitin was from Dako, and mouse monoclonal anti-GFP was from Roche Applied Science. Goat anti-mouse IgG-Cy3 was purchased from Molecular Probes and horseradish peroxidase-conjugated anti-mouse and anti-rabbit IgG were from Amersham Biosciences.

Expression Plasmids and Stable Cell Lines—The enhanced green fluorescence protein (EGFP) and tNhtt expression constructs, pIND-tNhtt-EGFP-16Q, pIND-tNhtt-150Q, and the generation of the stable cell lines of these constructs have been described previously (12). The construction of plasmids, pEGFP-N1-MJD(f)-20CAG and pEGFP-N1-MJD(f)-130CAG, pEGFP-N1-MJD(t)-20CAG, and pEGFP-N1-MJD(t)-80CAG were described elsewhere (13). The full-length CHIP cDNA was isolated from the total RNA extracted from HeLa cells by reverse transcription-PCR. Construction of full-length and the U-box-deleted CHIP in pcDNA vector with v5 tag were made using PCR.

Cell Culture, Transfection, Cell Viability Assay, and Counting of Aggregates—The wild type mouse neuro2a cells were cultured in Dulbecco's modified Eagle's medium supplemented with 10% heat-inactivated fetal bovine serum and the antibiotics penicillin/streptomycin. The stable cell lines (HD 16Q and HD 150Q) were maintained in the

[1] The abbreviations used are: HD, Huntington's disease; UPP, ubiquitin proteasome pathway; tNhtt, truncated N-terminal huntingtin; MTT, 3-(4,5-dimethylthiazol-2-yl)-2,5-diphenyltetrazolium bromide; dbcAMP, $N^6,2'$-O-dibutyryl-adenosine-3':5'-cyclic monophosphate; GFP, green fluorescent protein; EGFP, enhanced GFP; HSC, heat shock cognate.
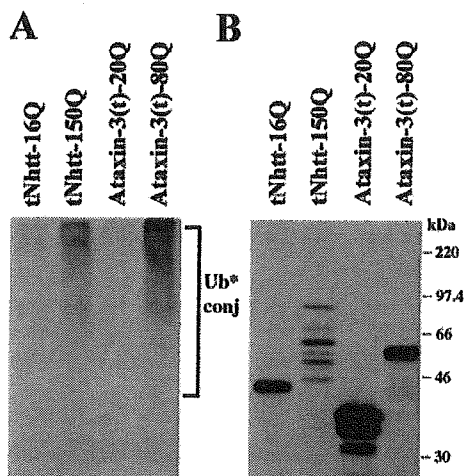
         CHIP Promotes Degradation of Polyglutamine Protein

FIG. 1. **Ubiquitination of expanded polyglutamine proteins.** The HD 16Q and HD 150Q cell lines were induced with 1 μM ponasterone A, or the truncated ataxin-3-EGFP fusion constructs with 20Q and 80Q were transiently transfected (1 μg of each/well of 6-well tissue-cultured plate) to the neuro2a cells. Twenty-four hours after induction or transfection, cell lysate were made and subjected to immunoprecipitation as described under "Experimental Procedures." Blots were probed sequentially with ubiquitin antibody (A) and GFP antibody (B). *Ub * conj*, ubiquitin conjugates.

same medium containing 0.4 mg/ml Zeocin and 0.4 mg/ml G418. One day prior to transfection, cells were plated into 6-well tissue-cultured plates at a subconfluent density. Cells were transiently transfected with expression vectors using Lipofectamine 2000 reagent according to the manufacturer's instruction. Transfection efficiency was ~80–90%. After 24 or 48 h of transfection, cells were used for immunofluorescence staining, co-immunoprecipitation, and immunoblotting. For cell viability assay, cells were first transfected with different expression plasmids. Twelve hours later, cells were harvested and replated into 96-well plates (5 × 10^3 cells/well). The cells were then differentiated with 5 mM dbcAMP and induced with 1 μM ponasterone A for 3 days. Cell viability was measured by MTT assay as described previously (12). Statistical analysis was performed using Student's t test, and $p < 0.05$ was considered to indicate statistical significance. Aggregate formation was manually counted under a fluorescence microscope (~500 transfected cells in each case), and the cells containing more than one aggregate were considered to have a single aggregate.

Co-immunoprecipitation and Immunoblotting Experiment—After 24 or 48 h of transfection, cells were washed with cold phosphate-buffered saline, scraped, pelleted by centrifugation, and lysed on ice for 30 min with radioimmune precipitation assay buffer (10 mM Hepes (pH 7.4), 150 mM NaCl, 10 mM EDTA, 2.5 mM EGTA, 1% Triton X-100, 0.1% SDS, 1% sodium deoxycholate, 10 mM NaF, 5 mM Na$_4$P$_2$O$_7$, 0.1 mM Na$_2$VO$_5$, 1 mM phenylmethylsulfonyl fluoride, 0.1 mg/ml Aprotinin). Cell lysates were briefly sonicated, centrifuged for 10 min at 15,000 × g at 4 °C, and the supernatants (total soluble extract) were used for immunoprecipitation as described earlier (9). For each immunoprecipitation experiment, 200 μg of protein in 0.2 ml of radioimmune precipitation assay buffer was incubated either with 5 μl (2 μg) of GFP antibody or 4 μl (2 μg) of normal mouse IgG. Bound proteins were eluted from the beads with SDS (1×) sample buffer, vortexed, boiled for 5 min, and analyzed by immunoblotting according to the procedure described earlier (9). Blot detection was carried out with enhanced chemiluminescence reagent. All primary antibodies were used in 1:1000 dilutions for immunoblotting.

Immunofluorescence Techniques—Cells grown in chamber slides or in 6-well tissue cultured plates were transiently transfected with different constructs. Forty-eight hours after transfection, cells were washed twice with phosphate-buffered saline, fixed with 4% paraformaldehyde in phosphate-buffered saline for 20 min, permeabilized with 0.5% Triton X-100 in phosphate-buffered saline for 5 min, washed extensively, then blocked with 5% nonfat dried milk in TBST (50 mM Tris, pH 7.5, 0.15 M NaCl, 0.05% Tween) for 1 h. Primary antibody (anti-v5, 1:5000 dilutions) incubation was carried out overnight at 4 °C. After several washings with TBST, cells were incubated with Cy3-conjugated secondary antibody (1:500 dilutions) for 1 h, washed several
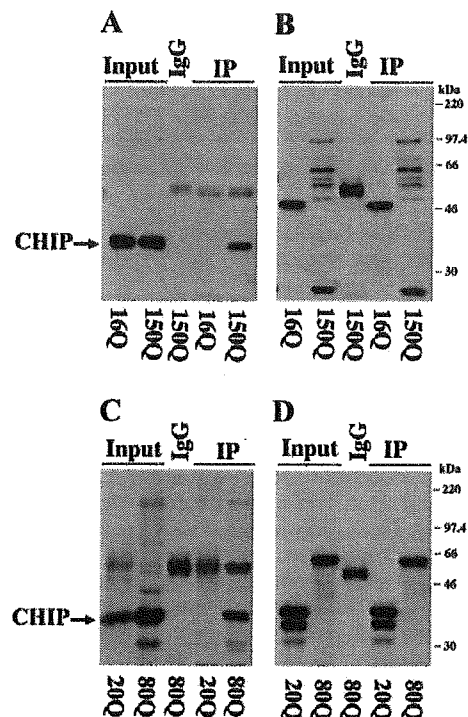

FIG. 2. **Interaction of CHIP with the expanded polyglutamine proteins.** A and B, the HD 16Q and HD 150Q cell lines were transiently transfected with CHIP (2 μg/well of 6-well tissue-cultured plate), and 12 h after transfection, media were changed, and the cells were induced with 1 μM ponasterone A. Twenty-four hours after induction, cells were collected and processed for immunoprecipitation (IP) by anti-GFP. Blots were sequentially probed with anti-v5 (A) and anti-GFP (B). C and D, neuro2a cells were first transfected with CHIP (2 μg/well of 6-well tissue-cultured plate). Twelve hours after first transfection, the medium was changed, and the cells were transfected again with the truncated ataxin-3-EGFP fusion constructs (1 μg of each/well) containing 20Q and 80Q. Twenty-four hours after the transfection of ataxin-3 constructs, cell lysates were made and subjected to immunoprecipitation as described in A and B. The blots were sequentially probed with anti-v5 (C) and anti-GFP (D).

times, and mounted in antifade solution. Samples were observed using a confocal microscope (Fluoview, Olympus), and digital images were assembled using Adobe Photoshop.

Degradation Assay—Neuro2a cells were plated in a 6-well tissue-cultured plate, and on the following day, cells were transiently transfected with full-length ataxin-3 with 20Q and 130Q with or without CHIP. Twenty-four hours post-transfection, cells were chased with 10 μg/ml of cycloheximide for different time periods. Cells collected at each time point were then processed for immunoblotting by anti-GFP.

RESULTS

Misfolded Truncated N-terminal Huntingtin or Ataxin-3 Are Ubiquitinated—We developed several stable neuro2a cell lines in an inducible system, that express tNhtt with normal (16Q) and expanded polyglutamine (150Q) (12). These cell lines were named HD 16Q and HD 150Q, and their corresponding expressed proteins were named tNhtt-16Q and tNhtt-150Q. The cell lines were induced for 1 day with ponasterone A (1 μM) and then processed for immunoprecipitation by anti-GFP. In another experiment, we transfected the truncated ataxin-3 constructs to the neuro2a cell, and after 1 day, cells were collected and processed for immunoprecipitation by GFP antibody. Blots were sequentially probed with anti-ubiquitin and anti-GFP. As shown in Fig. 1A, truncated huntingtin with 150Q proteins or the truncated ataxin-3 with 80Q proteins were ubiquitinated, whereas those truncated proteins with normal glutamine repeats were not ubiquitinated. Fig. 1B showed the same blot as those in A after probing with GFP antibody. The tNhtt-150Q
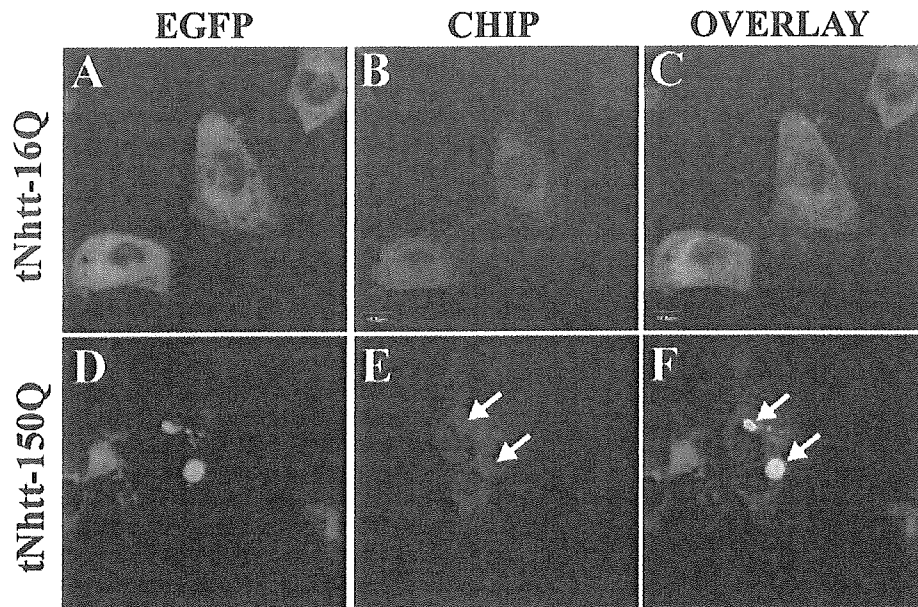
EGFP CHIP OVERLAY

FIG. 3. **Recruitment of CHIP to the mutant huntingtin aggregates.** The HD 16Q (*A–C*) and HD 150Q (*D–F*) cells were transiently transfected with CHIP and induced in the similar way as described in the Fig. 2. Cells were then subjected to immunofluorescence staining with anti-v5. Cy3-conjugated secondary antibody was used to stain the CHIP. *Arrows* indicate the recruitment of CHIP to the huntingtin aggregates.
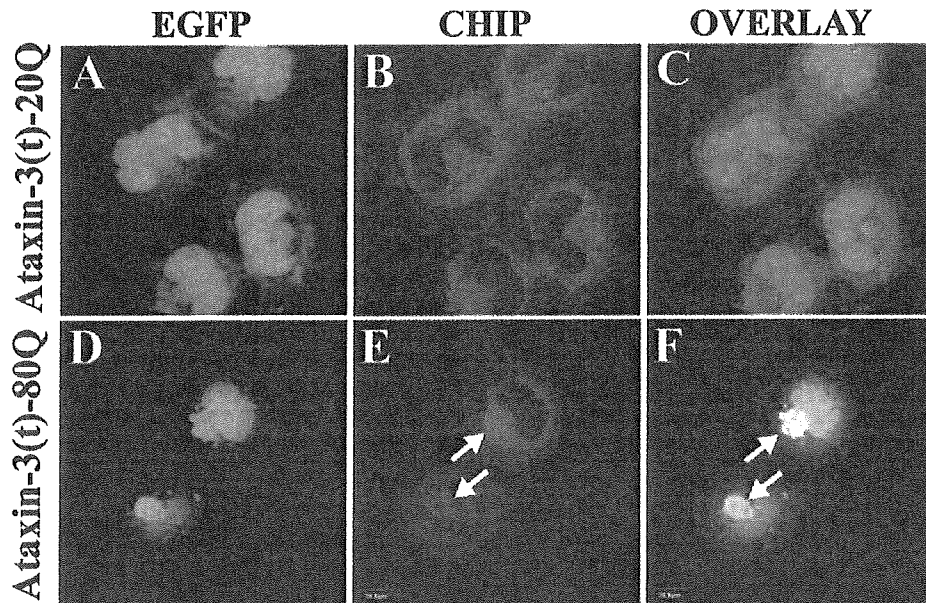
EGFP CHIP OVERLAY

FIG. 4. **CHIP associates with the ataxin-3 aggregates.** The neuro2a cells were sequentially transfected with CHIP and truncated ataxin-3-EGFP fusion constructs containing 20Q (*A–C*) and 80Q (*D–F*). Forty-eight hours later, cells were processed for immunofluorescence staining using v5 antibody. Cy3-conjugated secondary antibody was used to stain the CHIP. *Arrows* indicate the recruitment of CHIP to the ataxin-3 aggregates.

appeared as multiple bands because of the instability of the CAG repeats.

CHIP Interacts with the Polyglutamine-expanded Truncated N-terminal Huntingtin or Ataxin-3—Because misfolding promotes the ubiquitination of the expanded polyglutamine proteins, we next wanted to know the identity of the ubiquitin ligase that is responsible for the misfolding-dependent ubiquitination. We first tested the possibility of CHIP ubiquitin ligase, because recently, CHIP has been shown to be responsible for the ubiquitination and degradation of the misfolded proteins. CHIP was transiently transfected into HD 16Q and HD 150Q cells, the cells were induced with ponasterone A for 1

day, and then the cell lysates were processed for immunoprecipitation by anti-GFP. In a similar experiment, CHIP was co-transfected along with a different truncated ataxin-3 construct, and then the cell lysates were processed for immunoprecipitation. In both experiments, blots were detected with anti-v5 antibody. As shown in Fig. 2, *A* and *C*, CHIP was immunoprecipitated with the truncated N-terminal huntingtin with 150Q and truncated ataxin-3 with 80Q but not the truncated N-terminal huntingtin with 16Q or truncated ataxin-3 with 20Q. Fig. 2, *B* and *D* showed the same blot as in Fig. 2, *A* and *C*, respectively, after detection with anti-GFP.

Association of CHIP with Polyglutamine Aggregates—Next

A   B

Ub*
conj.

Blot:
anti-Ub

Ub*
conj.

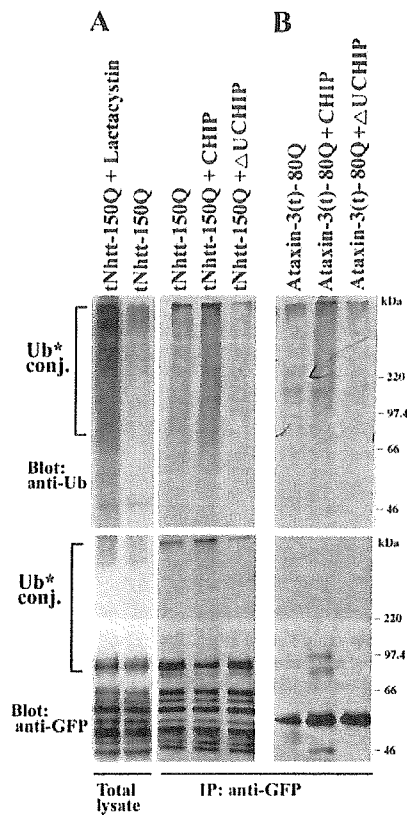Blot:
anti-GFP

Total   IP: anti-GFP
lysate

FIG. 5. **Involvement of CHIP in the ubiquitination of expanded polyglutamine proteins.** *A*, the HD 150Q cells were transiently transfected with full-length CHIP, U-box-deleted CHIP or the empty vectors (2 μg of each/well of 6-well tissue-cultured plate) and induced and processed for immunoprecipitation (*IP*) in the similar way as described in the Fig. 2. Blots were sequentially probed with anti-ubiquitin (*top blot*) and anti-GFP (*bottom blot*). In total lysate lanes, induced HD 150Q cells were left untreated or treated with 10 μM lactacystin for 8 h, and then the cell lysate were made and subjected to immunoblotting. *B*, neuro2a cells were first transfected with full-length CHIP, U-box-deleted CHIP, and empty vector (same amounts as used in *A*), and after 12 h, the cells were transfected again with truncated ataxin-3 constructs with 20Q and 80Q in the similar way as described in Fig. 2. The cell lysate were then processed for immunoprecipitation by anti-GFP followed by sequential immunoblotting with anti-ubiquitin (*top blot*) anti-GFP (*bottom blot*). *Ub* conj*, ubiquitin conjugates.

we checked the normal distribution and recruitment of CHIP to the polyglutamine aggregates. First we transiently transfected the CHIP into the HD 16Q and HD 150Q cells, and then the cells were induced to express the truncated huntingtin proteins. After 1 day of induction, cells were processed for immunofluorescence experiments using anti-v5 antibody. CHIP was normally localized into the cytosolic compartment in the wild type neuro2a cells or in the uninduced HD 16Q and HD 150Q cells (Fig. 3). Induction of the expression of the tNhtt-16Q protein did not alter the localization pattern of CHIP in the HD 16Q cell; however, the induction of tNhtt-150Q protein in the HD 150Q cell caused the recruitment of CHIP to the aggregates (Fig. 3). Next, we tested the similar redistribution of CHIP in the ataxin-3 aggregates. CHIP was co-transfected along with truncated ataxin-3 constructs and after 2 days of transfection, cells were processed for immunofluorescence experiments. As expected, CHIP was also recruited to truncated ataxin-3 aggregates (Fig. 4).

CHIP Enhances the Ubiquitination of Polyglutamine-expanded Truncated N-terminal Huntingtin or Ataxin-3—Because CHIP co-immunoprecipitates with expanded polyglutamine proteins and recruits the polyglutamine aggregates, we further tested its possible involvement in the ubiquitination of the expanded polyglutamine proteins. To test this hypothesis, we transfected CHIP (both full-length and U-box-deleted) to the HD 150Q cells, or co-transfected CHIP along with truncated ataxin-3 constructs. The cell lysate were then made and processed for immunoprecipitation by anti-GFP. Fig. 5 showed that CHIP enhanced the rate of ubiquitination of both truncated N-terminal huntingtin containing 150Q (Fig. 5A, *top blot*) as well as truncated ataxin-3 with 80Q (Fig. 5B, *top blot*). This enhanced rate of ubiquitination was prevented by the deletion of U-box of CHIP. The bottom blots of both Fig. 5, *A* and *B* are the same blots as the top blots, respectively, but probed with anti-GFP. Anti-GFP also detected smears of ubiquitinated derivatives of expanded polyglutamine proteins in the only CHIP-transfected cell lysate. The lactacystin-treated cell lysate was used as positive control to compare the CHIP-induced ubiquitination profile (Fig. 5A, *first two lanes*). Because the deletion of U-box of CHIP reduced the rate of ubiquitination, we further tested whether the U-box-deleted CHIP still associates with the polyglutamine aggregates. As shown in Fig. 6, U-box deleted CHIP also recruits to the huntingtin aggregates. We have also observed the association of U-box-deleted CHIP with the

EGFP   ΔU CHIP   Overlay

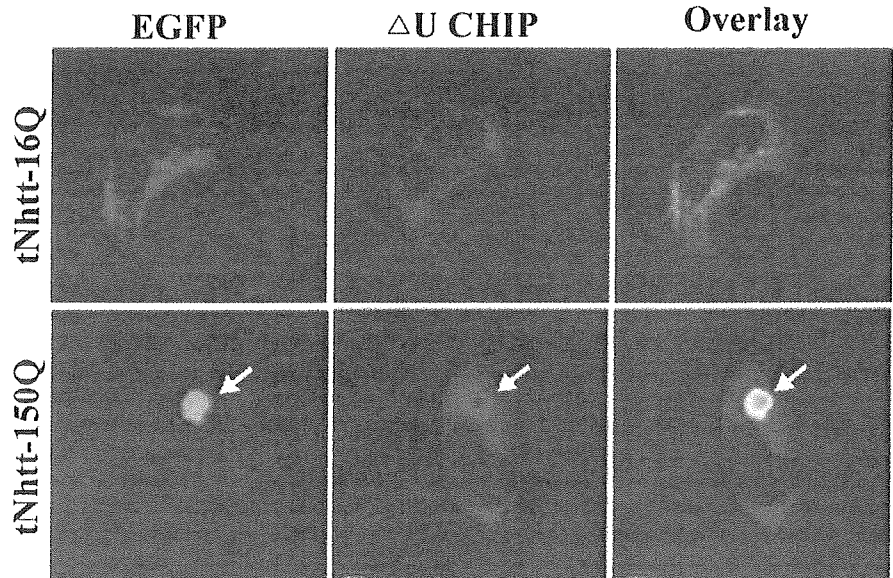FIG. 6. **Association of U-box-deleted CHIP with the huntingtin aggregates.** The HD 16Q and HD 150Q cells were transiently transfected with U-box-deleted CHIP and induced in a similar way as described in the Fig. 2. Cells were then subjected to immunofluorescence staining with anti-v5. Cy3-conjugated secondary antibody was used to stain the CHIP. *Arrows* indicate the recruitment of U-box deleted CHIP to the huntingtin aggregates.
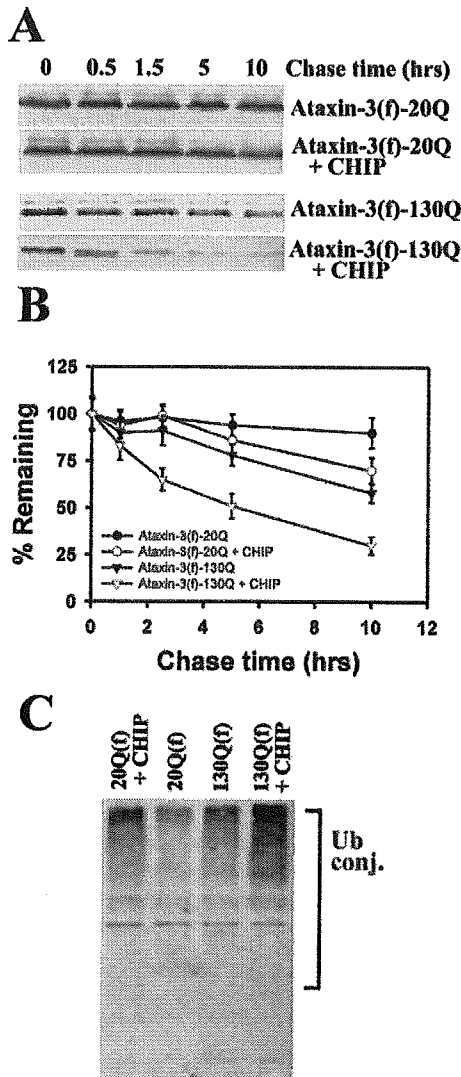
A

| 0 | 0.5 | 1.5 | 5 | 10 | Chase time (hrs) |

Ataxin-3(f)-20Q

Ataxin-3(f)-20Q + CHIP

Ataxin-3(f)-130Q

Ataxin-3(f)-130Q + CHIP

B

% Remaining vs Chase time (hrs)

- —●— Ataxin-3(f)-20Q
- —○— Ataxin-3(f)-20Q + CHIP
- —▼— Ataxin-3(f)-130Q
- —▽— Ataxin-3(f)-130Q + CHIP

C

20Q(f) + CHIP | 20Q(f) | 130Q(f) | 130Q(f) + CHIP

Ub conj.

FIG. 7. CHIP promotes degradation of polyglutamine-expanded proteins. *A*, mouse neuro2a cells were transiently transfected with full-length ataxin-3 constructs (20Q and 130Q) either alone or along with CHIP. Twenty-four hours later, cells were chased in the presence of 10 μg/ml cycloheximide for different time periods as indicated in the figure. Cells were then collected and processed for immunoblotting using anti-GFP. *B*, quantitation of the band intensities of the blots collected from three independent experiments were performed using NIH Image analysis software. Values are means ± S.D. *C*, cells were transfected as described in *A*. Cells were collected and subjected to immunoprecipitation using anti-GFP. Blot was detected with anti-ubiquitin. *Ub* conj*, ubiquitin conjugates.

ataxin-3 aggregates (data not shown). Result strongly indicates that the CHIP associates with the expanded polyglutamine protein through its interaction with Hsc70.

CHIP Enhances the Degradation of Polyglutamine-expanded Proteins—Because CHIP enhanced the ubiquitination of polyglutamine-expanded proteins; we further checked their rate of degradation upon CHIP overexpression. For this experiment, we used full-length ataxin-3 with 20Q and 130Q, because full-length ataxin-3 with 130Q forms very few aggregates (~5–10% cells form aggregates) after 48 h of transfection. Neuro2a cells were transiently transfected with ataxin-3 constructs either alone or along with CHIP. Twenty-four hours later, cells were chased with cycloheximide. As shown in Fig. 7, *A* and *B*, full-length ataxin-3 with 20Q is not degraded; however, full-length ataxin-3 with 130Q is degraded after 1.5, 5, and 10 h of chase.
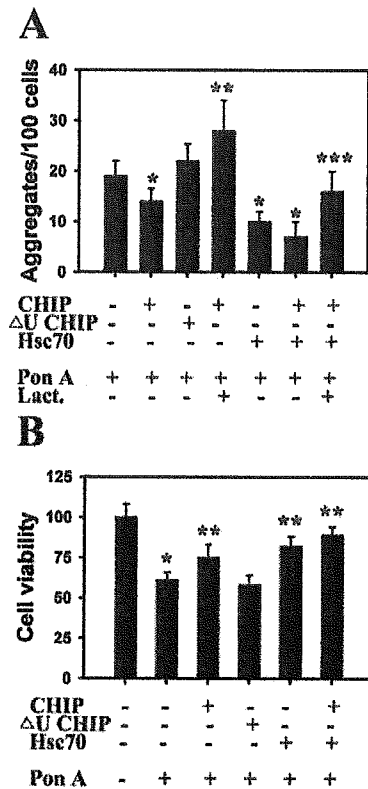
A

CHIP	-	+	-	+	-	+	+
ΔU CHIP	-	-	+	-	-	-	-
Hsc70	-	-	-	-	+	+	+
Pon A	+	+	+	+	+	+	+
Lact.	-	-	-	+	-	-	+

B

CHIP	-	-	+	-	-	+
ΔU CHIP	-	-	-	+	-	-
Hsc70	-	-	-	-	+	+
Pon A	-	+	+	+	+	+

FIG. 8. CHIP reduces the aggregate formation (*A*) and cell death (*B*) caused by expanded polyglutamine protein. *A*, HD 150Q cells were transiently transfected with CHIP and U-box-deleted (Δ*U*) CHIP independently or together with Hsc70 (2 μg of each/well of 6-well tissue-cultured plate). Transfected DNA was equalized by using empty pcDNA vector. Twelve hours later, the medium was replaced, and then the cells were induced with 0.5 μM ponasterone A (*Pon A*). Aggregate counting was monitored 24 h after ponasterone A treatment in the fluorescence microscope as described under "Experimental Procedures." Lactacystin (*Lact.*) was used at a dose of 2.5 μM. Results are means ± S.D. of three independent experiments each performed triplicate. *, $p < 0.05$ as compared with control; **, $p < 0.01$ as compared with CHIP-transfected experiment; ***, $p < 0.01$ as compared with CHIP plus Hsc70-transfected experiment. *B*, HD 150Q cells were transiently transfected with CHIP and U-box deleted CHIP independently or together with Hsc70 as described under *A*. Cells were harvested and replated in the 96-well tissue cultured plate. The cells were then differentiated with 5 mM dbcAMP and induced with 1 μM ponasterone A for 3 days. Cell viability was measured by MTT assay. Values are means ± S.D. of two independent experiments each performed triplicate. *, $p < 0.01$ as compared with control; **, $p < 0.01$ as compared with ponasterone A treated experiments.

Overexpression of CHIP enhanced the degradation of full-length ataxin-3 with 130Q. Overexpression of CHIP also slightly enhanced the degradation of ataxin-3 with 20Q (Fig. 7, *A* and *B*). Fig. 7*C* demonstrated that full-length ataxin-3 with 130Q was ubiquitinated, and CHIP overexpression enhanced the rate of ubiquitination.

CHIP Decreases the Aggregation and Cell Death Mediated by the Expanded Polyglutamine Proteins—Because CHIP promotes the ubiquitination of expanded polyglutamine proteins, we expected that its overexpression would increase the rate of degradation of expanded polyglutamine proteins by proteasomes. If so, CHIP should decrease the aggregation of polyglutamine proteins. Therefore, we next checked the effect of CHIP on the rate of aggregate formation and cell viability in the HD 150Q cells after different days of transfection. As shown in Fig. 8*A*, overexpression of CHIP reduced the polyglutamine-expanded tNhtt aggregation, and the suppressive effect is more prominent when the CHIP is overexpressed along with Hsc70.

The deletion of the U-box of the CHIP abolished the suppressive effect on aggregation. CHIP overexpression also decreased the aggregation of truncated ataxin-3 with 80Q (data not shown). This inhibitory effect of CHIP on aggregate formation was prevented by the proteasome inhibitor lactacystin. CHIP was also able to protect the polyglutamine protein-induced cell death, and again, the protective effect was more when the CHIP was overexpressed along with Hsc70 (Fig. 8B).

DISCUSSION

Ubiquitin is a well known marker of polyglutamine aggregates, but how and when polyglutamine aggregates are ubiquitinated is not yet known. The most likely hypothesis is that the expanded polyglutamine proteins are misfolded, and failure to refold might cause their ubiquitination before they are degraded by proteasome. Here we first demonstrated that the expanded polyglutamine proteins that are misfolded became ubiquitinated. Secondly, we identified CHIP ubiquitin ligase that is responsible for the misfolding-dependent ubiquitination of the expanded polyglutamine proteins. Finally, we showed that overexpression of CHIP reduces the aggregate formation and cell death mediated by expanded polyglutamine proteins.

Ubiquitination begins with the ATP-dependent activation of ubiquitin by an activating enzyme (E1). The ligation of ubiquitin to the substrate is then carried out by a specific complex composed of an ubiquitin-conjugating enzyme (E2) and ubiquitin protein ligase (E3) (14). The question now is how the misfolded polyglutamine protein is recognized by the ubiquitination machine and whether chaperones play any role. The expanded polyglutamine protein has been shown earlier to specifically interact with Hsc70/Hsp70 chaperones (9), and now we have shown that CHIP associates and ubiquitinates expanded polyglutamine proteins. Results suggest that the Hsc70/Hsp70 and CHIP both play a critical role in the process of ubiquitination of polyglutamine proteins. CHIP was first identified as an interacting protein with the C terminus of Hsp70 and shown to negatively regulated Hsp70 chaperone activity (15). Subsequently, CHIP was demonstrated to be a ubiquitin ligase of the U-box family (16, 17). Recent reports also demonstrated that CHIP is responsible for the misfolding-dependent ubiquitination and degradation of cystic fibrosis transmembrane regulator (18), glucocorticoid receptor (19), mutant copper/zinc superoxide dismutase 1 (20, 21), and Tau protein (22, 23) and therefore could be a general ubiquitin ligase for the misfolded proteins (24, 25).

We have also observed that the overexpression of CHIP inhibits polyglutamine protein aggregation and cell death and that the inhibitory effects are more prominent when CHIP is expressed along with the Hsc70 chaperone. The results suggests that polyglutamine proteins are degraded by proteasomes after they are ubiquitinated by CHIP and that the removal of polyglutamine proteins protects cells from their toxic effect. Others have reported similar findings (20–23) where they have shown that overexpression of CHIP reduced the aggregation and cell death mediated by mutant copper/zinc superoxide dis-

mutase 1 or Tau protein. However, there are reports suggesting that the expanded polyglutamine proteins are not degraded efficiently by the proteasome and that also there is proteasomal malfunction in the expanded polyglutamine protein-expressing cells (11, 26). In both the cases, there could be an increased accumulation of ubiquitinated derivatives of expanded polyglutamine proteins. CHIP along with Hsc70 might enhance the rate of degradation by increasing the ubiquitination rate. Overexpression of CHIP along with Hsc70 could also conceivably have recovered proteasomal malfunction by reducing the burden of aggregated polyglutamine proteins as well as other misfolded proteins. Altogether, our results demonstrate that the CHIP along with Hsc70 promotes the ubiquitination and degradation of expanded polyglutamine proteins that ultimately leads to the suppression of aggregation and cell death.

REFERENCES

1. Zoghbi, H. Y., and Orr, H. T. (2000) *Ann. Rev. Neurosci.* **23**, 217–247
2. Sherman, M. Y., and Goldberg, A. L. (2001) *Neuron* **29**, 15–32
3. Lin, X., Cummings, C. J., and Zoghbi, H. Y. (1999) *Neuron* **24**, 499–502
4. Cummings, C. J., Mancini, M. A., Antalffy, B., DeFranco, D. B., Orr, H. T., and Zoghbi, H. Y. (1998) *Nat. Genet.* **19**, 148–154
5. Chai, Y., Koppenhafer, S. L., Shoesmith, S. J., Perez, M. K., and Paulson, H. L. (1999) *Hum. Mol. Genet.* **8**, 673–682
6. Chai, Y., Koppenhafer, S. L., Bonini, N. M., and Paulson, H. L. (1999) *J. Neurosci.* **19**, 10338–10347
7. Stenoien, D. L., Cummings, C. J., Adams, H. P., Mancini, M. G., Patel, K., DeMartino, G. N., Marcelli, M., Weigel, N. L., and Mancini, M. A. (1999) *Hum. Mol. Genet.* **8**, 731–741
8. Warrick, J. M., Chan, H. Y. E., Gray-Board, G. L., Chai, Y., Paulson, H. L., and Bonini, N. M. (1999) *Nat. Genet.* **23**, 425–428
9. Jana, N. R., Tanaka, M., Wang, G., and Nukina, N. (2000) *Hum. Mol. Genet.* **9**, 2009–2018
10. Cummings, C. J., Reinstein, E., Sun, Y., Antalffy, B., Jiang, Y-H., Ciechanover, A., Orr, H. T., Beaudet, A. L., and Zoghbi, H. (1999) *Neuron* **24**, 879–892
11. Jana, N. R., Zemskov, E. A., Wang, G., and Nukina, N. (2001) *Hum. Mol. Genet.* **10**, 1049–1059
12. Wang, G. H., Mitsui, K., Kotliarova, S. E., Yamashita, A., Nagao, Y., Tokuhiro, S., Iwatsubo, T., Kanazawa, I., and Nukina, N. (1999) *Neuroreport* **10**, 2435–2438
13. Wang, G. H., Sawai, N., Kotliarova, S. E., Kanazawa, I., and Nukina, N. (2000) *Hum. Mol. Genet.* **9**, 1795–1803
14. Ciechanover, A. (1998) *EMBO J.* **17**, 7151–7160
15. Ballinger, C. A., Connell, P., Wu, Y., Hu, Z., Thompson, L. J., Yin, L. Y., and Patterson, C. (1999) *Mol. Cell. Biol.* **19**, 4535–4545
16. Jiang, J., Ballinger, C. A., Wu, Y., Dai, Q., Cyr, D. M., Hohfeld, J., and Patterson, C. (2001) *J. Biol. Chem.* **276**, 42938–42944
17. Hatakeyama, S., Yada, M., Matsumoto, M., Ishida, N., and Nakayama, K. I. (2001) *J. Biol. Chem.* **276**, 33111–33120
18. Meacham, G. C., Patterson, C., Zhang, W., Younger, J. M., and Cyr, D. M. (2001) *Nat. Cell Biol.* **3**, 100–105
19. Connell, P., Ballinger, C. A., Jiang, J., Wu, Y., Thompson, L. J., Hohfeld, J., and Patterson, C. (2001) *Nat. Cell Biol.* **3**, 93–96
20. Choi, J. S., Cho, S., Park, S. G., Park, B. C., and Lee, D. H. (2004) *Biochem. Biophys. Res. Commun.* **321**, 574–583
21. Urushitani, M., Kurisu, J., Tateno, M., Hatakeyama, S., Nakayama, K., Kato, S., and Takahashi, R. (2004) *J. Neurochem.* **90**, 231–244
22. Petrucelli, L., Dickson, D., Kehoe, K., Taylor, J., Snyder, H., Grover, A., De Lucia, M., McGowan, E., Lewis, J., Prihar, G., Kim, J., Dillman, W. H., Browne, S. E., Hall, A., Voellmy, R., Tsuboi, Y., Dawson, T. M., Wolozin, B., and Hardy, J. H. (2004) *Hum. Mol. Genet.* **13**, 703–714
23. Hatakeyama, S., Katsumoto, M., Kamura, T., Murayama, M., Chui, D. H., Planel, E., Takahashi, R., Nakayama, K. I., and Takashima, A. (2004) *J. Neurochem.* **91**, 299–307
24. Demand, J., Alberti, S., Patterson, C., and Hohfeld, J. (2001) *Curr. Biol.* **11**, 1569–1577
25. Murata, S., Minami, Y., Minami, M., Chiba, T., and Tanaka, K. (2001) *EMBO Rep.* **2**, 1133–1138
26. Holmberg, C. I., Staniszewski, K. E., Mensah, K. N., Matouschek, A., Morimoto, R. I. (2004) *EMBO J.* **23**, 307–318

UV-Induced Ubiquitylation of XPC Protein Mediated by UV-DDB-Ubiquitin Ligase Complex

Kaoru Sugasawa,[1,2,9,*] Yuki Okuda,[1,3,9]
Masafumi Saijo,[2,4] Ryotaro Nishi,[1,2,3,4]
Noriyuki Matsuda,[5] Gilbert Chu,[6] Toshio Mori,[7]
Shigenori Iwai,[8] Keiji Tanaka,[5] Kiyoji Tanaka,[2,4]
and Fumio Hanaoka[1,2,4]
[1]Cellular Physiology Laboratory
RIKEN Discovery Research Institute
[2]Core Research for Evolutional Science
 and Technology
Japan Science and Technology Agency
Wako, Saitama 351-0198
[3]Graduate School of Pharmaceutical Sciences
[4]Graduate School of Frontier Biosciences
Osaka University
Suita, Osaka 565-0871
[5]Department of Molecular Oncology
Tokyo Metropolitan Institute of Medical Science
Bunkyo-ku, Tokyo 113-8613
Japan
[6]Department of Medicine and Biochemistry
Stanford University
Stanford, California 94305
[7]Radioisotope Center
Nara Medical University
Kashihara, Nara 634-8521
[8]Graduate School of Engineering Science
Osaka University
Toyonaka, Osaka 560-8531
Japan

Summary

The xeroderma pigmentosum group C (XPC) protein complex plays a key role in recognizing DNA damage throughout the genome for mammalian nucleotide excision repair (NER). Ultraviolet light (UV)-damaged DNA binding protein (UV-DDB) is another complex that appears to be involved in the recognition of NER-inducing damage, although the precise role it plays and its relationship to XPC remain to be elucidated. Here we show that XPC undergoes reversible ubiquitylation upon UV irradiation of cells and that this depends on the presence of functional UV-DDB activity. XPC and UV-DDB were demonstrated to interact physically, and both are polyubiquitylated by the recombinant UV-DDB-ubiquitin ligase complex. The polyubiquitylation altered the DNA binding properties of XPC and UV-DDB and appeared to be required for cell-free NER of UV-induced (6-4) photoproducts specifically when UV-DDB was bound to the lesion. Our results strongly suggest that ubiquitylation plays a critical role in the transfer of the UV-induced lesion from UV-DDB to XPC.

*Correspondence: sugasawa@riken.jp
[9]These authors contributed equally to this work.

Introduction

Nucleotide excision repair (NER) is a versatile DNA repair pathway that eliminates a wide variety of helix-distorting base lesions, including ultraviolet light (UV)-induced cyclobutane pyrimidine dimers (CPDs) and pyrimidine-pyrimidone (6-4) photoproducts (6-4PPs), as well as bulky adducts induced by numerous chemical compounds. Impaired NER activity is associated with several rare autosomal recessive disorders in humans, such as xeroderma pigmentosum (XP) and Cockayne syndrome (CS) (Friedberg, 2001; Hoeijmakers, 2001). XP patients are clinically characterized by cutaneous hypersensitivity to sunlight exposure and a predisposition to skin cancer. Seven NER-deficient genetic complementation groups of XP (XP-A to -G) and two groups of CS (CS-A and -B) have been identified, and all of the corresponding genes (XPA~XPG, CSA, and CSB) have now been cloned (for a review, see Bootsma et al. [1997]).

Mammalian NER consists of two distinct subpathways: global genome NER (GG-NER), which operates throughout the genome, and transcription-coupled NER (TC-NER), which specifically removes lesions on the transcribed DNA strand of active genes. A major difference between these two subpathways appears to be in the strategies they use to detect damaged bases. In TC-NER, RNA polymerase II stalls at damage sites and triggers the repair reaction (Tornaletti and Hanawalt, 1999). In contrast, in GG-NER, protein factors bind specifically to damage sites. Accumulating evidence indicates that the XP group C (XPC) protein plays an essential role in GG-NER-specific damage recognition (Riedl et al., 2003; Sugasawa et al., 1998; Volker et al., 2001).

The XPC protein exists in vivo as a heterotrimeric complex with one of the two mammalian homologs of S. cerevisiae Rad23p (HR23A or HR23B) and centrin 2 (Araki et al., 2001; Masutani et al., 1994; Shivji et al., 1994). This complex binds to various NER-type lesions in vitro, including UV-induced 6-4PP (Batty et al., 2000; Sugasawa et al., 2001). However, biochemical studies revealed that the XPC complex is a structure-specific DNA binding factor that appears to recognize a certain secondary structure of DNA rather than the lesions themselves (Sugasawa et al., 2002). These biochemical properties of XPC plausibly explain the detection by GG-NER of many structurally unrelated lesions.

UV-damaged DNA binding protein (UV-DDB) has been also implicated in the lesion recognition of GG-NER. UV-DDB is a heterodimeric complex consisting of DDB1 (p127) and DDB2 (p48). It has a much higher binding affinity and specificity for damaged DNA than XPC (Batty et al., 2000), particularly with regard to UV-induced 6-4PP (Fujiwara et al., 1999; Reardon et al., 1993; Treiber et al., 1992). Mutations in the DDB2 gene cause the genetic complementation group E of XP, and the patients belonging to this group lack the damage binding activity of UV-DDB (Chu and Chang, 1988;

Hwang et al., 1998; Itoh et al., 2000; Nichols et al., 1996; Rapic'-Otrin et al., 2003).

Despite its capacity for detecting DNA damage with extremely high sensitivity, UV-DDB is not required for all types of GG-NER. For example, the cell-free NER reaction was successfully reconstituted without UV-DDB (Araújo et al., 2000; Mu et al., 1995), although it has stimulatory effects under certain conditions (Abous-sekhra et al., 1995; Wakasugi et al., 2001; Wakasugi et al., 2002). However, in XP-E cells lacking UV-DDB activity, while GG-NER of 6-4PP is only moderately impaired, the removal of CPD from the global genome is profoundly reduced (Hwang et al., 1999). Furthermore, ectopic expression of functional human DDB2 in rodent cells enhances GG-NER of CPD, thereby suppressing UV-induced mutagenesis (Tang et al., 2000). These findings strongly suggest that UV-DDB plays an important role in recognizing CPD for GG-NER. Upon local UV irradiation within the nucleus, UV-DDB translocates into the damaged area even in the absence of XPC (Waka-sugi et al., 2002), suggesting that UV-DDB may function at an earlier step in GG-NER in order to assist XPC to find damaged sites. However, it remains to be elucidated how XPC and UV-DDB are functionally linked in terms of damage recognition for GG-NER. The precise role of the extremely high binding affinity UV-DDB has for 6-4PP also remains unclear.

Interestingly, UV-DDB has recently been found to be contained in a large complex with cullin 4A, Roc1, and COP9 signalosome, which are components of ubiquitin ligase (E3) (Groisman et al., 2003). Although UV-DDB-associated E3 appears to be activated upon UV irradiation of cells, the physiological substrates of E3 activity have not yet been determined. Here we present evidence that the UV-DDB-E3 complex ubiquitylates XPC in response to UV irradiation of cells. Our findings functionally link the two NER damage recognition factors and provide novel insights into the molecular mechanisms underlying damage recognition in GG-NER.

Results

UV-Induced Posttranslational Modification of XPC Protein

To examine the in vivo response of the XPC complex to UV irradiation, a series of immunoblot analyses was carried out. The SV40-transformed, normal human fibroblast cell line WI38 VA13 was UV or mock irradiated and then lysed with buffer containing 0.3 M NaCl and 1% Nonidet P40. When the resulting soluble and insoluble fractions were subjected to immunoblotting with anti-XPC antibodies (Figure 1A, lanes 1–4), slowly migrating heterogeneous bands (150–300 kDa) appeared in the soluble fraction from the UV-irradiated cells (lane 2). These bands with lower mobility were detected with two anti-XPC antibodies of different specificity but did not appear in similar fractions prepared from the XPC-deficient cell line XP4PASV (lanes 5–8). These findings indicate that the XPC protein undergoes posttranslational modification in response to UV irradiation of the cells.

To investigate the time course of this XPC band shift, WI38 VA13 cells were UV irradiated and then incubated

for various time periods before cell fractionation. In this experiment, the cells were cultured in the presence of cycloheximide to inhibit de novo protein synthesis after UV irradiation. We confirmed that treatment of the cells with 0.1 mM cycloheximide inhibited the incorporation of [^{3}H]leucine almost completely within 1 hr (data not shown). As shown in Figure 1B, slowly migrating XPC species appeared as early as 5 min after irradiation, peaked around 60 min, and declined thereafter. In the same set of cell extracts, no detectable band shift was observed for HR23B, XPA, XPB, or DDB1 (Figure 1B) or for centrin 2 (data not shown).

The response of XPC in cells treated with various DNA-damaging agents other than UV was also examined (see Figure S1 in the Supplemental Data available with this article online). The shift in molecular weight of XPC upon treatment with X-rays or chemicals such as 4-nitroquinoline 1-oxide (4-NQO), which is often referred to as a UV mimetic agent, was either undetectable or much weaker than that induced by UV. The observed XPC modification thus appeared to be rather specific for UV irradiation.

The XPC Protein Is Ubiquitylated In Vivo

The observed mobility shift of XPC upon UV irradiation was large and heterogeneous, with apparent sizes differing by 20 to more than 100 kDa. This pattern raised the possibility that ubiquitylation might be involved in this band shift. To test this possibility, the UV-induced XPC modification was examined with mouse FM3A ts85 mutant cells, which have been shown to express a temperature-sensitive form of the ubiquitin-activating enzyme E1 (Finley et al., 1984; Matsumoto et al., 1983). When cultured at nonpermissive temperatures (>39°C), de novo ubiquitylation is greatly reduced in these cells. In agreement with this, the levels of monoubiquitylated histone H2A (uH2A) are severely reduced in ts85 cells cultured at 39.5°C (Figure 1D, lanes 10–12) but not in the mutant cells maintained at permissive temperatures (lanes 7–9) or in the wild-type, parental FM3A cells cultured at either temperature (lanes 1–6). The UV-induced band shift of XPC was not detected in ts85 cells cultured at 39.5°C (Figure 1D). Thus, the UV-induced modification of XPC depends on E1 activity.

To demonstrate the ubiquitylation of XPC more directly, we first established a stable transformant of the XPC-deficient cell line XP4PASV that expresses FLAG-tagged XPC at physiological levels. This FLAG-XPC protein showed a shift in molecular weight after UV irradiation that exactly matched the change in endogenous XPC in UV-irradiated WI38 VA13 cells (Figure S2A). In addition, GG-NER of 6-4PP was completely restored in this transformant (Figure S2B), confirming that the expressed FLAG-XPC functions normally in vivo. Hemagglutinin (HA)-tagged ubiquitin was transiently overexpressed in this transformant, and FLAG-XPC was immunoprecipitated. When the precipitated samples were subjected to immunoblotting with anti-HA antibody, ubiquitylated FLAG-XPC was detected, particularly when the transfected cells were UV irradiated before the extract preparation (Figure 1E, lane 8). A low level of ubiquitylation may have occurred in the unirradiated cells, presumably because of nonspecific ubiq-
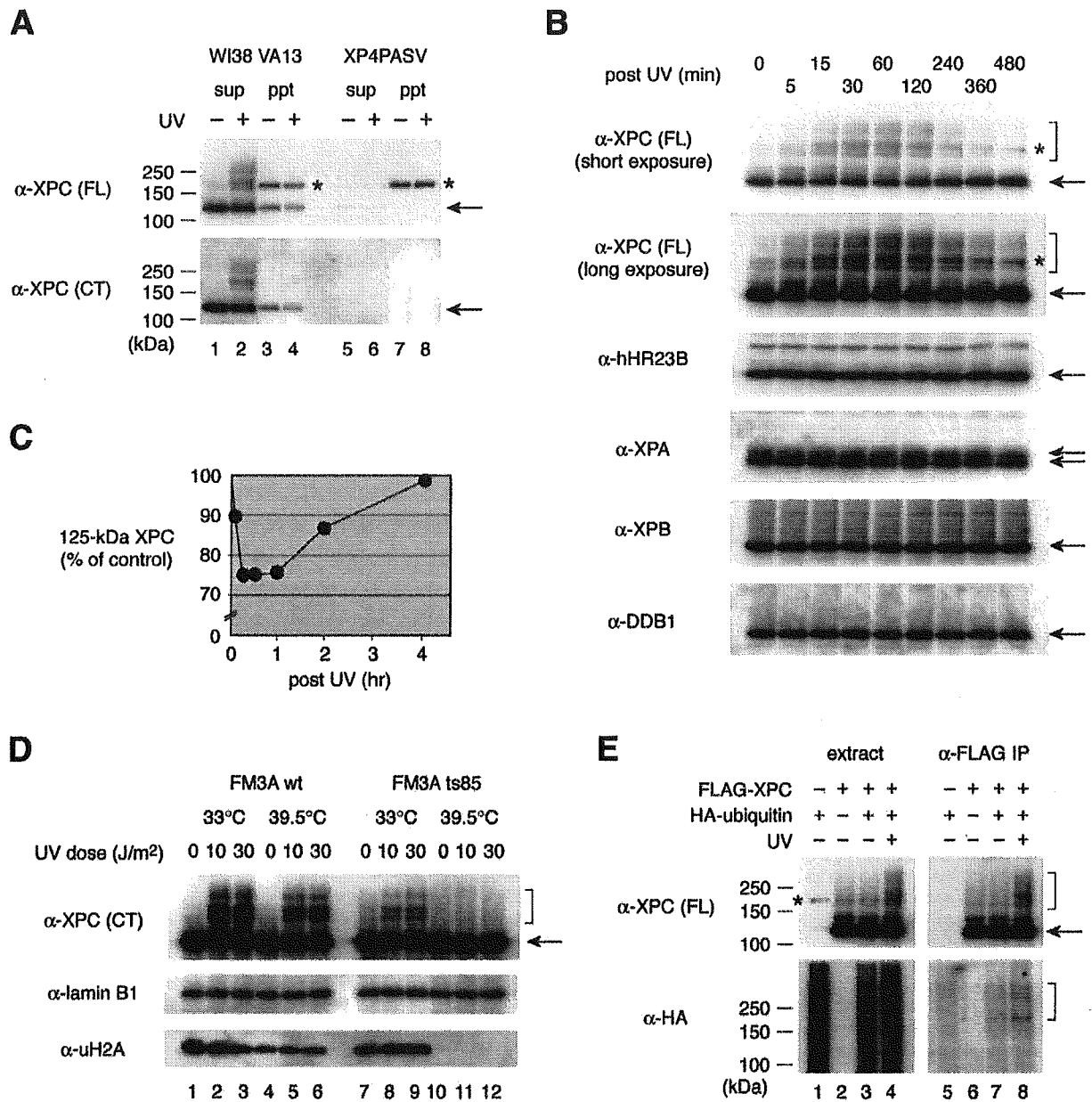
Figure 1. XPC Is Ubiquitylated in Response to UV Irradiation

(A) WI38 VA13 (normal) and XP4PASV (XPC-deficient) cells were UV irradiated at 10 J/m² or mock irradiated. After incubation at 37°C for 1 hr, soluble (sup) cell extracts, each containing 3 μg protein, as well as the corresponding amounts of the insoluble (ppt) fractions were subjected to immunoblot analyses using two different anti-XPC antibodies raised against the full-length (FL) protein or against a synthetic peptide corresponding to the C terminus (CT). The asterisk (also the asterisks in [B] and [E]) indicates nonspecific bands that crossreact with the anti-XPC (FL) antibody. The arrows (also the arrows in [D] and [E]) indicate the authentic unmodified XPC bands.

(B) WI38 VA13 cells were UV irradiated at 10 J/m² and incubated at 37°C in the presence of 0.1 mM cycloheximide for various times as indicated. The soluble cell lysates, each containing 3 μg protein, were subjected to immunoblot analyses with various antibodies as indicated. The arrows indicate the authentic bands for each NER protein. The brackets (also those in [D] and [E]) indicate the modified forms of XPC.

(C) The levels of 125 kDa XPC in each lane in (B) were quantified and normalized relative to the amount of hHR23B in the same lane. These values then were further normalized by the initial amount of the 125 kDa band and plotted as a graph.

(D) FM3A wild-type or ts85 cells were cultured for 16 hr at 33°C or 39.5°C, UV irradiated at the indicated doses, and cultured for another hour at the same temperature. Cell lysates were subjected to immunoblot analyses using the anti-XPC (CT) antibody. The same lysates were also immunoblotted for lamin B1 as a loading control and monoubiquitylated histone H2A (uH2A).

(E) The transformed XP4PASV cell line that stably expressed FLAG-XPC at physiological levels (XP4PASV/fXPC) was transiently transfected with an expression vector for HA-ubiquitin. Controls consisted of untransfected parental XP4PASV cells (lanes 1 and 5) and XP4PASV cells transfected with the vacant pCAGGS vector (lanes 2 and 6). At 7 hr of posttransfection, the cells were UV irradiated at 10 J/m² and incubated for another hour. Soluble cell extracts were prepared and subjected to immunoprecipitation with anti-FLAG M2 agarose. Aliquots of the cell extracts (3 μg protein; lanes 1–4) as well as the immunoprecipitates (lanes 5–8) were subjected to immunoblot analyses using the indicated antibodies.
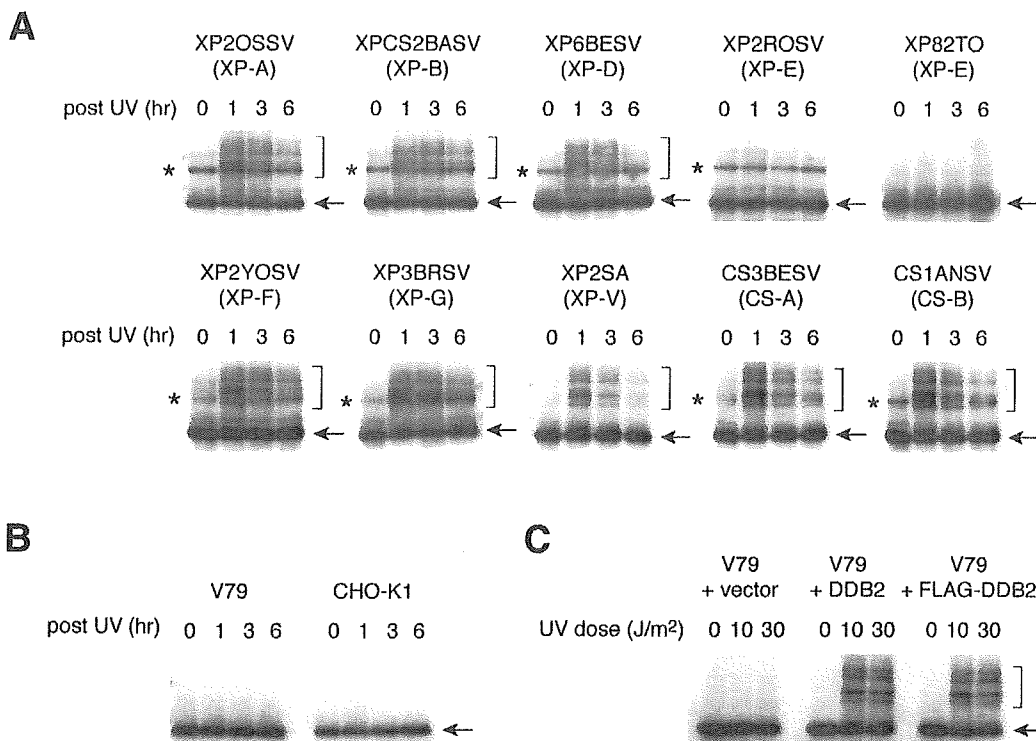
Figure 2. UV-Induced XPC Modification Depends on the Presence of Functional UV-DDB

(A) Cell lines derived from different XP and CS genetic complementation groups were UV irradiated at 10 J/m^2 and incubated at 37°C in the presence of 0.1 mM cycloheximide for various time periods. The soluble cell extracts (3 µg protein) were subjected to immunoblotting with anti-XPC (FL) antibody. The asterisks indicate nonspecific crossreacting bands that appear more evident in SV40-transformed cell lines than in the two untransformed cell lines XP82TO and XP2SA. The arrows and brackets (also those in [B] and [C]) indicate unmodified and modified forms of XPC, respectively.

(B) The Chinese hamster cell lines V79 and CHO-K1 were UV irradiated and cultured as described in (A). Cell lysates were prepared and subjected to immunoblot analysis using the anti-XPC (CT) antibody.

(C) Stable V79 transformants expressing human DDB2 (either untagged or FLAG-tagged), as well as a control transformant containing the vacant expression vector, were UV irradiated at the indicated doses and incubated at 37°C for 1 hr. Cell lysates were subjected to immunoblot analyses as described in (B).

uitylation caused by the overexpression of HA-ubiquitin (lane 7). From these data, we conclude that UV irradiation induces the ubiquitylation of XPC.

We found that, even when de novo protein synthesis was inhibited, the total amount of XPC was not significantly reduced after UV irradiation (Figure 1B). When we measured the levels of the authentic 125 kDa band of XPC, we found its levels dropped upon UV irradiation and then rose again later on when the shifted bands disappeared (Figure 1C). Therefore, the ubiquitylation of XPC appears to be reversible and does not serve as a signal for degradation.

UV-DDB Is Required for the Modification of XPC

To explore possible relationships between XPC modification and the NER process, we examined the UV-induced shift in molecular weight of XPC in human cell lines belonging to different genetic complementation groups of XP and CS. As shown in Figure 2A, most of the mutant cells exhibited normal band shifting of XPC upon UV irradiation. Intriguingly, however, the XPC band shift was not induced in two independent XP-E

cell lines (Figure 2A). Both of these cells have mutations in the DDB2 gene and lack UV-DDB activity (Nichols et al., 1996).

To further investigate the involvement of UV-DDB in XPC modification, Chinese hamster cell lines were used. Many established cell lines as well as primary lymphoid cells derived from Chinese hamsters lack UV-DDB activity (Hwang et al., 1998; Tang et al., 2000). As shown in Figure 2B, the two Chinese hamster cell lines we used, V79 and CHO-K1, were also defective in the UV-induced shift in molecular weight of XPC. UV-DDB activity is conferred to V79 cells when human DDB2 gene is stably expressed (Tang et al., 2000). Interestingly, when human DDB2 (untagged or FLAG-tagged) was expressed in V79 cells, the XPC modification upon UV irradiation was restored (Figure 2C). We also confirmed that transient expression of wild-type human DDB2 but not its two point mutants (K244E and R273H) identified from XP-E patients complemented the defect of UV-induced XPC band shift in XP2ROSV cells (data not shown). These results indicate that UV-DDB activity is necessary for the UV-induced modification of XPC.
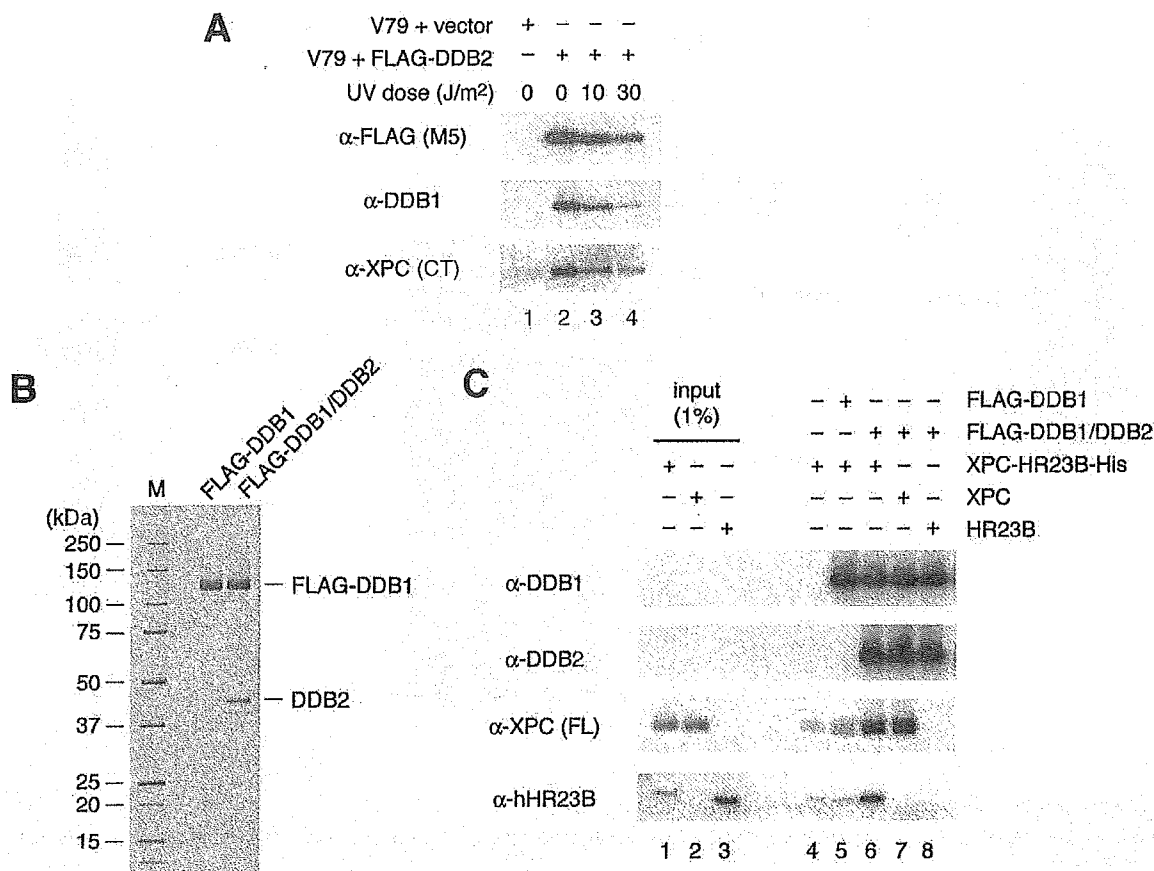
Figure 3. XPC Physically Interacts with UV-DDB

(A) The V79 transformant expressing FLAG-DDB2 was UV irradiated at the indicated dose (lanes 2–4). After incubation at 37°C for 1 hr, soluble cell extracts were prepared, FLAG-DDB2 was immunoprecipitated with anti-FLAG antibody beads, and aliquots of the bound fractions were subjected to immunoblot analyses with the indicated antibodies. As a negative control, the unirradiated, V79 transformant containing the vacant expression vector was processed in the same way (lane 1).

(B) Purification of recombinant UV-DDB. Purified FLAG-DDB1 (150 ng) and FLAG-DDB1/DDB2 heterodimer (200 ng) were subjected to SDS-PAGE (with a 4%–20% gradient gel) followed by silver staining. M, molecular weight markers.

(C) Anti-FLAG antibody beads (20 μl) prebound to either FLAG-DDB1 (1.3 μg) or FLAG-DDB1/DDB2 (1.8 μg) were incubated with XPC-HR23B-His (150 ng), XPC alone (103 ng), or HR23B alone (47 ng). After unbound materials were washed out, aliquots of the bound proteins were subjected to immunoblot analyses using the indicated antibodies (lanes 4–8). One percent of the input XPC and/or HR23B proteins were loaded onto the same gel as controls (lanes 1–3).

UV-DDB Physically Interacts with XPC

The above findings indicating some functional interaction between XPC and UV-DDB prompted us to examine whether they interacted physically as well. When FLAG-DDB2 in the stable V79 transformant was immunoprecipitated from soluble cell extracts, both DDB1 and endogenous XPC were coprecipitated (Figure 3A). This suggests that UV-DDB indeed interacts with XPC in vivo. This interaction was present in both unirradiated and irradiated cells, although UV irradiation significantly reduced the amount of UV-DDB and XPC that was precipitated. This is probably because UV-DDB becomes tightly bound to the UV-induced lesions and thus is not soluble during the extraction procedure (Otrin et al., 1997).

To demonstrate a direct interaction between XPC and UV-DDB, binding experiments were carried out using purified recombinant proteins. FLAG-DDB1 and DDB2 proteins were coexpressed in insect cells using the baculovirus system. With our baculovirus construct, FLAG-DDB1 was expressed in a large excess over DDB2, enabling us to separately purify the FLAG-DDB1/DDB2 complex and free FLAG-DDB1 from the same infected cell extract (Figure 3B). Either the purified UV-DDB complex or FLAG-DDB1 was bound to anti-FLAG antibody beads, which were then incubated with purified XPC-HR23B-His complex. A significant amount of XPC-HR23B-His coprecipitated with the UV-DDB complex, while its binding to FLAG-DDB1 alone was close to background levels (Figure 3C, compare lane 6 with lanes 4 and 5). This indicates that DDB2 is required for the interaction of UV-DDB with XPC. When XPC and HR23B were added separately to the UV-DDB heterodimer, only XPC was detected in the bound frac-
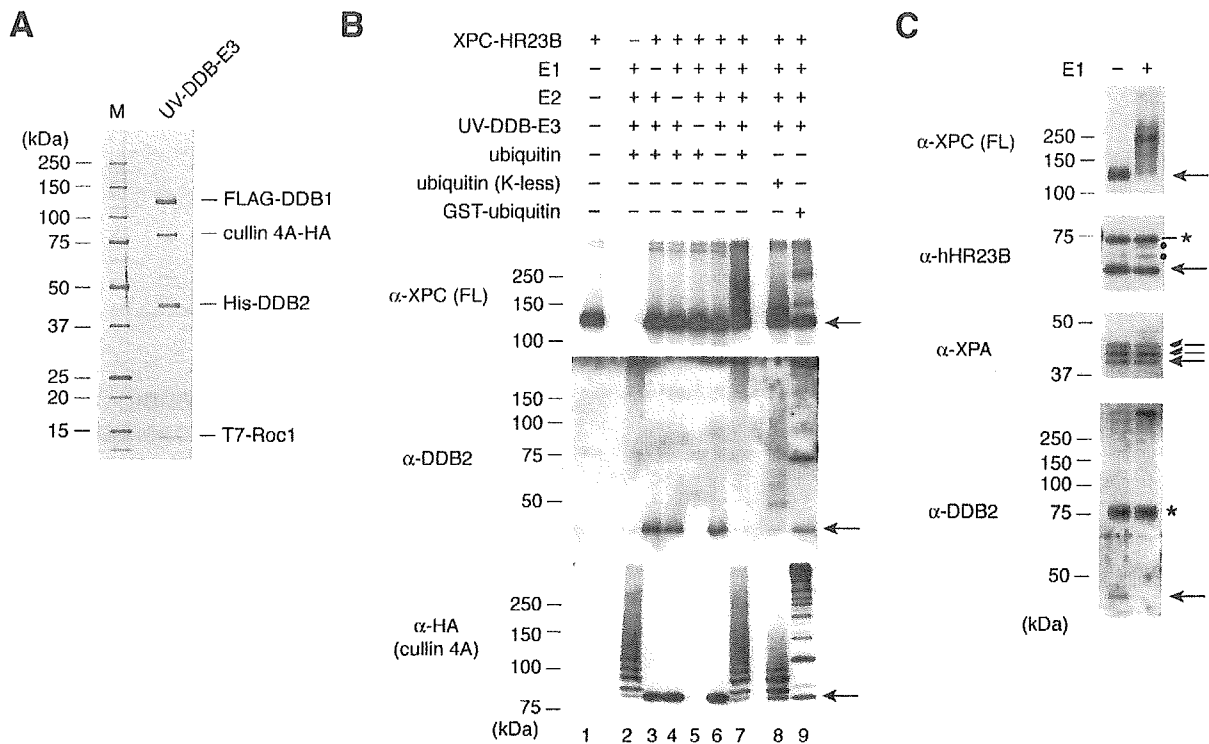
Figure 4. Cell-Free Ubiquitylation of XPC Mediated by the UV-DDB-E3 Complex

(A) The purified UV-DDB-E3 complex was subjected to SDS-PAGE (with a 4%–20% gradient gel) followed by silver staining. M, molecular weight markers.

(B) Cell-free ubiquitylation reactions were performed using the indicated sets of protein components. Where indicated, K-less ubiquitin (5 μg) or GST-ubiquitin (10 μg) was included instead of wild-type ubiquitin (lanes 8 and 9). Aliquots of the reaction mixtures were subjected to immunoblot analyses using the indicated antibodies. The arrows (also those in [C]) indicate the unmodified form of each protein.

(C) A mixture of XPC-HR23B-His (8 ng) and FLAG-XPA (5 ng) was included in the ubiquitylation reaction described in (B) in the absence or presence of E1. Aliquots of the reaction mixtures were subjected to immunoblotting with the indicated antibodies. The asterisk indicates nonspecifically crossreacting bands. The bands indicated by dots represent HR23B-His that had undergone low levels of ubiquitylation.

tion (lanes 7 and 8). These data demonstrate a direct physical interaction between XPC and UV-DDB.

The UV-DDB-E3 Complex Catalyzes the Ubiquitylation of XPC In Vitro

It has been recently reported that UV-DDB exists in vivo as a supercomplex containing cullin 4A and Roc1 that displays ubiquitin ligase (E3) activity (Groisman et al., 2003). This, together with our data, strongly suggests that the UV-DDB-E3 complex may be responsible for the ubiquitylation of XPC. To test this idea, cell-free ubiquitylation assays were carried out. The four subunits (DDB1, DDB2, cullin 4A, and Roc1) were expressed simultaneously in insect cells, and the heterotetrameric complex was purified (Figure 4A). When XPC-HR23B-His was incubated with this UV-DDB-E3 complex in the presence of E1, E2 (UbcH5a), ubiquitin, and ATP, a shift in the molecular weight of XPC was detected (Figure 4B). The shift appeared to depend on each of the protein components (lanes 2–7). The use of GST-tagged ubiquitin instead of normal ubiquitin resulted in an altered pattern of the shifted XPC bands (lane 9), strongly suggesting that the observed band shift is due to conjugation to ubiquitin. Furthermore,

when a mutant ubiquitin in which all the lysine residues were changed to arginines (designated "K-less" ubiquitin) was employed in the reaction, the band shift was significantly reduced (lane 8), suggesting that the slow mobility species shown in lane 7 were the result of polyubiquitin chain formation. In the same reactions, DDB2 and cullin 4A were found to be ubiquitylated extensively as well, regardless of the presence or absence of XPC-HR23B-His (Figure 4B, lanes 2 and 7).

To examine the specificity of this in vitro ubiquitylation, XPC-HR23B-His and FLAG-XPA were simultaneously included in the reaction. While XPC and DDB2 were ubiquitylated extensively, little band shifting was observed with FLAG-XPA (Figure 4C) and DDB1 (data not shown) in the same reaction. Although a low percentage of HR23B-His appeared to be conjugated to one or two ubiquitin moieties (see bands indicated by dots in Figure 4C), the band shifting was nonetheless much less pronounced than XPC and DDB2. Thus, the in vitro ubiquitylation system appeared to retain similar substrate specificity as observed in the UV-irradiated cells (Figure 1B).

Since XPC and DDB2 were ubiquitylated in vitro by the same E3 complex, the in vivo fates of the two proteins after UV irradiation were compared. To do this,

we used the V79 transformant expressing FLAG-DDB2, since the available anti-DDB2 antibodies cannot detect endogenous DDB2 expressed in human cells with sufficient sensitivity. When the cells were UV irradiated and incubated in the presence of cycloheximide, XPC underwent reversible modification (lanes 1–6 in Figure S3) exactly as observed in the WI38 VA13 cells. In contrast, the FLAG-DDB2 band decreased in a time-dependent manner and had disappeared almost completely by 4 hr of postirradiation. This decrease in FLAG-DDB2 was blocked when the cells were treated simultaneously with the proteasome inhibitor MG132 (lanes 7–12). Therefore, in agreement with the previous reports (Fitch et al., 2003a; Rapic'-Otrin et al., 2002), DDB2 appeared to be degraded after UV irradiation by the ubiquitin/proteasome system.

Ubiquitylation Alters the DNA Binding Properties of XPC and UV-DDB

To obtain insights into roles the ubiquitylation plays in NER, we examined the DNA binding properties of ubiquitylated XPC and UV-DDB. For this purpose, a synthetic oligonucleotide containing a single UV lesion (CPD or 6-4PP) or the undamaged sequence as a control (Figure S4A) was annealed to the complementary oligonucleotide, tandemly ligated, and immobilized on paramagnetic beads. Cell-free ubiquitylation reactions were carried out in the presence of one of these DNA beads. After unbound fractions were saved and the beads were washed, the proteins retained by the DNA were subjected to immunoblotting for detection of XPC as well as subunits of the UV-DDB-E3 complex (Figure 5A).

When XPC alone was incubated with the DNA beads, only a part of the input protein was detected in the bound fractions (lanes 1–3). We have shown previously (Sugasawa et al., 2001) and in Figure S4B by using the electrophoretic mobility shift assay that XPC specifically binds to 6-4PP and not to CPD, when XPC was added in excess over the damaged DNA; the addition of appropriate competitor DNA was also necessary to absorb the nonspecific DNA binding activity of XPC so that its binding specificity could be unveiled. The binding specificity of XPC for 6-4PP was not as evident in the DNA binding assay shown in Figure 5A, probably because the protein:DNA ratio was much lower and competitor DNA was not included. The presence of the UV-DDB-E3 complex did not affect the binding properties of XPC if ubiquitylation did not occur (Figure 5A, lanes 4–6). In the same reactions, both DDB1 and DDB2 were bound to the 6-4PP beads in a nearly quantitative manner (lane 6), while little binding was observed with the undamaged DNA beads (lane 4). Both the affinity and specificity of UV-DDB for 6-4PP thus seemed to be far higher than those of XPC. The binding of UV-DDB to CPD was also observed, although the affinity appeared to be much lower than that for 6-4PP, as expected from previous reports (Fujiwara et al., 1999; Reardon et al., 1993; Treiber et al., 1992) and our mobility shift assays (Figure S4C). In addition, a significant amount of cullin 4A remained in the unbound fraction even in the presence of the 6-4PP beads (Figure 5A, lane 6), suggesting a somewhat unstable association of the E3 subunit with the UV-DDB core.

Intriguingly, when all factors required for ubiquitylation were present, only ubiquitylated XPC was detected in the DNA bound fractions, although a significant part of XPC still remained unmodified in the unbound fraction (Figure 5A, lanes 7–9). It was also notable that the bands of XPC and cullin 4A were shifted into higher molecular weight regions in the presence of 6-4PP, unlike with undamaged DNA or CPD beads (compare lane 9 with lanes 7 and 8). Thus, although the addition of DNA was not essential for E3 activity (Figure 4), the presence of 6-4PP seemed to stimulate the UV-DDB-dependent ubiquitylation. In these reactions, DDB2 was extensively ubiquitylated, and very little DDB1 or DDB2 was detected in the bound fractions with any of the DNA beads (lanes 7–9). Thus, the ubiquitylation of UV-DDB abolished its DNA binding activity almost completely. In contrast, UV-DDB still retained its DNA binding activity as well as specificity for the UV lesions when methylated ubiquitin was included instead of normal ubiquitin (lanes 10–12), while DDB2 still showed significant band shifts. Reductive methylation of lysine residues in ubiquitin blocks the elongation of polyubiquitin chains (compare the patterns of band shifting in lanes 7–9 with those in lanes 10–12). These data indicate that the formation of polyubiquitin chains above a certain length abrogate the damage binding activity of UV-DDB, whereas polyubiquitylated XPC retains its ability to bind DNA.

To quantitatively examine the effects of ubiquitylation on the DNA binding of XPC, various amounts of XPC-HR23B-His were included in the reaction (Figure 5B). At all doses of XPC tested, ubiquitylation resulted in an about 2-fold increase in the XPC that was retained by DNA beads. However, this effect was observed with undamaged DNA beads as well as with 6-4PP beads (see quantitative data in Figure 5C) and CPD beads (data not shown). Therefore, ubiquitylation appeared to augment the DNA binding of XPC rather than to alter its specificity.

Effects of Ubiquitylation on Cell-Free NER Incision

Finally, we investigated the effects of the ubiquitylation mediated by the UV-DDB-E3 complex on the cell-free NER incision reaction. For this purpose, we prepared a whole-cell extract from the human lymphoblastoid cell line GM01646, which was derived from an XP group E patient. An internally ^{32}P-labeled double-stranded circular DNA substrate containing a single 6-4PP was first preincubated with various amounts of UV-DDB (FLAG-DDB1/DDB2 heterodimer). The mixtures were then incubated with the XP-E cell extract (100 μg of protein), and the labeled dual incision products containing the lesion were separated and detected by denaturing PAGE. As shown in Figure 6A, the preincubation with UV-DDB had little effect on the dual incision around 6-4PP in the cell extract under the conditions tested (lanes 1–4). However, when 20 μg of methylated ubiquitin was added, UV-DDB inhibited the repair of 6-4PP in a dose-dependent manner (lanes 9–12; see also quantitative data in Figure 6B). This inhibition was much less pronounced in the presence of the same amount of normal ubiquitin (lanes 5–8) but similar to when K-less ubiquitin was substituted for methylated ubiquitin (data
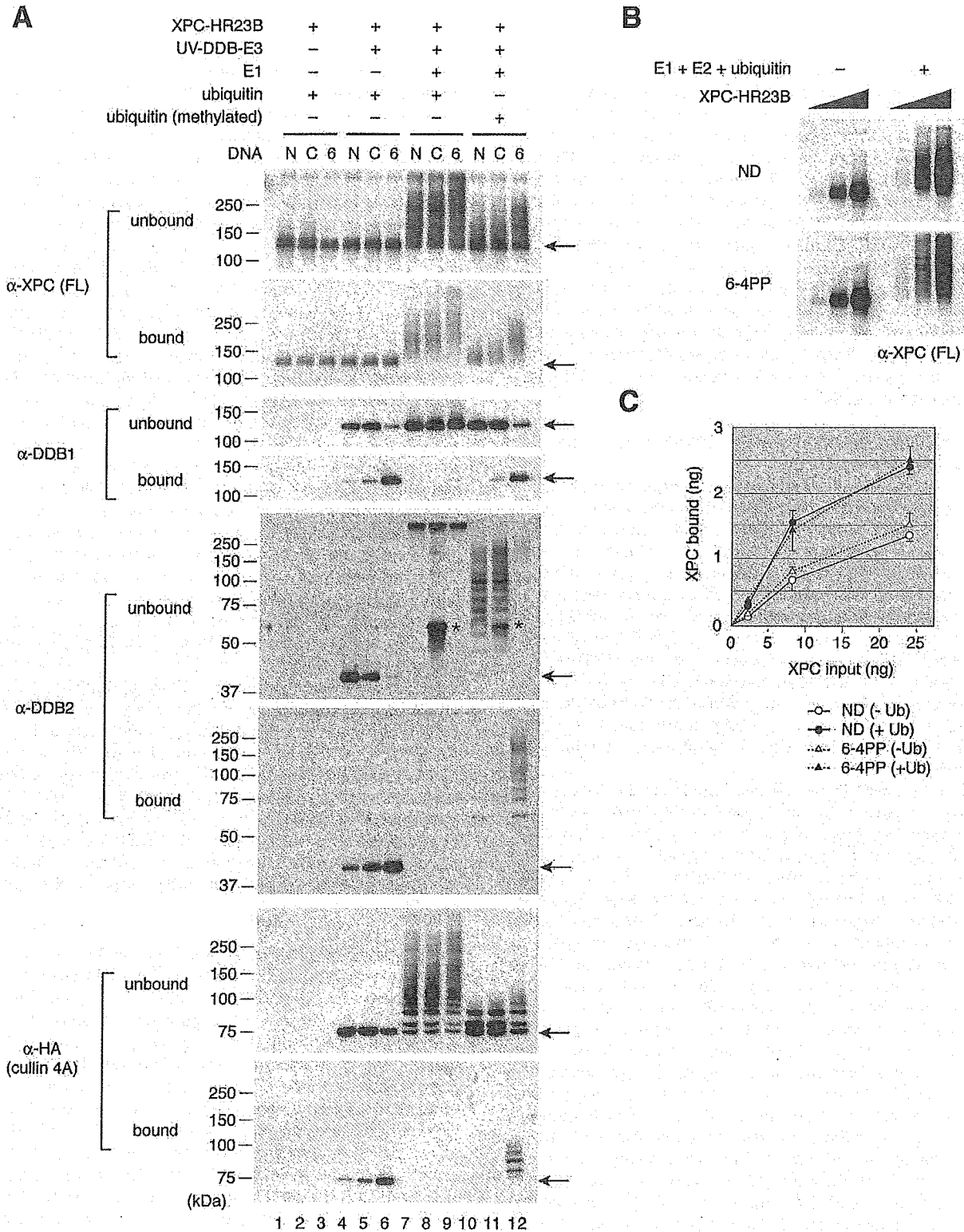
Figure 5. Ubiquitylation Alters the DNA Binding Properties of XPC and UV-DDB

(A) XPC-HR23B-His (8 ng) was incubated with paramagnetic beads bearing undamaged DNA (N) or DNA containing CPD (C) or 6-4PP (6). UV-DDB-E3 (20 ng), and other factors required for ubiquitylation were also included as indicated. The proteins that did not bind to DNA (unbound) and those retained by DNA (bound) were subjected to immunoblot analyses using the indicated antibodies. The arrows indicate the unmodified form of each protein. The asterisks indicate crossreacting bands derived from contaminating keratin.

(B) Binding reactions were performed with undamaged (ND) DNA beads or 6-4PP beads as described in (A) except that the XPC-HR23B-His levels varied (2.4, 8, and 24 ng). The XPC protein that was retained on the DNA beads is shown.

(C) The bound XPC levels in (B) were quantified by comparison with the signals of known amounts of XPC and plotted as a graph. The mean ± standard error of the mean was calculated from two independent experiments.
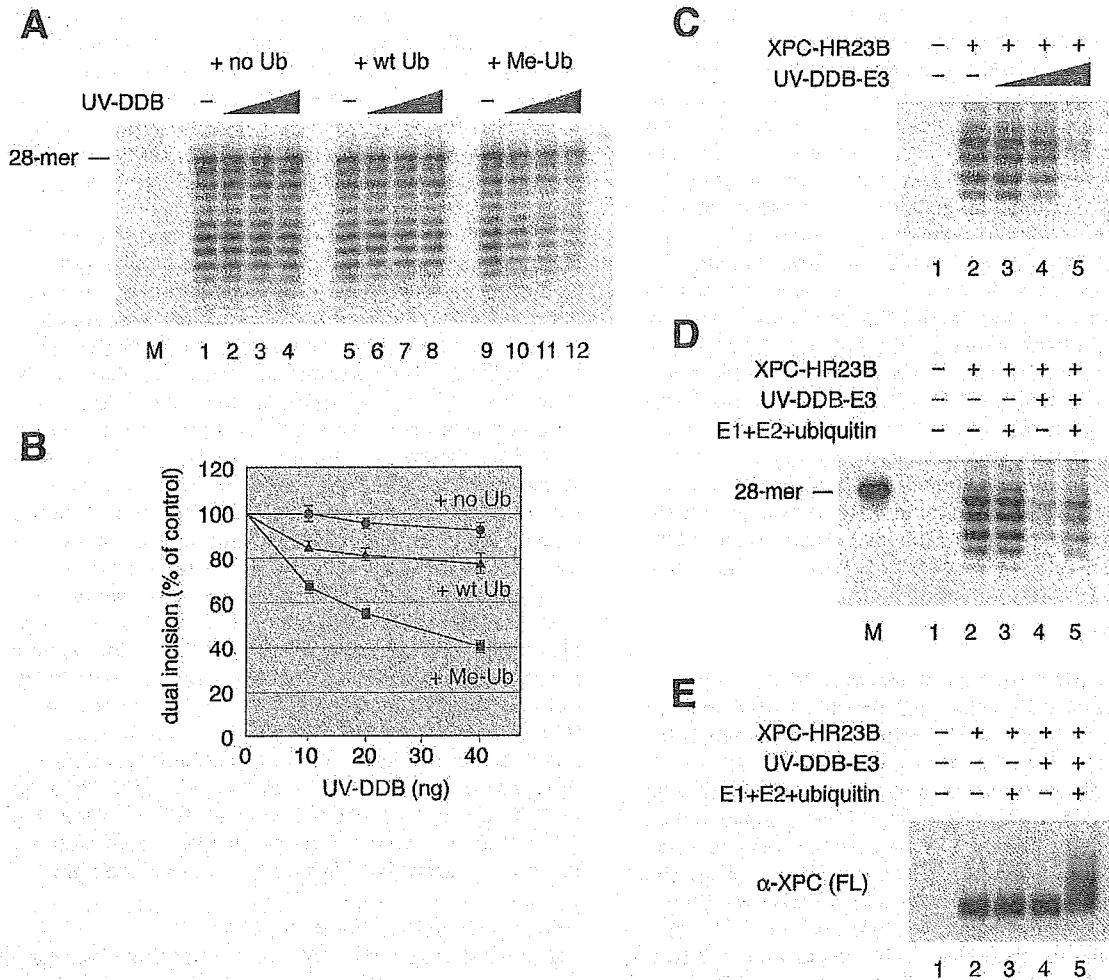
Figure 6. Effect of Ubiquitylation on Cell-Free NER Incision

(A) The internally ^{32}P-labeled DNA substrate containing a single 6-4PP was preincubated at 30°C for 10 min with various amounts of UV-DDB (FLAG-DDB1/DDB2 heterodimer; 10, 20, and 40 ng). The cell-free NER incision assay was then performed by adding the XP-E cell extract (100 μg protein) with or without 20 μg each of wild-type ubiquitin (wt Ub) or methylated ubiquitin (Me-Ub). Dual incision products detected on denaturing PAGE are shown. M, ^{32}P-labeled 28-mer oligonucleotide as a size marker (also for [D]).

(B) The levels of dual incision products for each lane in (A) were quantified, normalized relative to the value of the control reactions without UV-DDB, and plotted as a graph. The mean ± standard error of the mean was calculated from two independent experiments.

(C) Cell-free NER incision reactions were reconstituted with purified protein factors and carried out with the internally ^{32}P-labeled DNA substrate containing a single 6-4PP. Various amounts of purified UV-DDB-E3 (0.4, 4, and 40 ng) were also included (lanes 3–5). As a negative control, XPC-HR23B was omitted from the standard reaction (lane 1).

(D) Cell-free NER incision reactions were carried out with purified NER proteins in the presence or absence of UV-DDB-E3 (40 ng) and other factors required for ubiquitylation as indicated.

(E) The same set of reactions was carried out as described in (D), except that the unlabeled DNA substrate containing a 6-4PP was used. Aliquots of the reactions were subjected to immunoblotting with the anti-XPC (FL) antibody.

not shown). From a quantitative immunoblot analysis, we estimated that no more than 0.5 μg of endogenous, unconjugated ubiquitin was present in the extract included in a reaction (data not shown). Therefore, it was likely that the addition of K-less or methylated ubiquitin in such a large excess may competitively block the elongation of polyubiquitin chains. Immunoblot analyses revealed that UV-DDB-dependent polyubiquitylation of XPC indeed occurred in the NER reaction using the crude extract and that this was inhibited by the addition of K-less ubiquitin (Figure S5). The above results thus suggest that, when UV-DDB is bound to 6-4PP,

the formation of relatively long polyubiquitin chains is important for subsequent processing of the lesion by NER. Similar experiments were carried out with a DNA substrate containing CPD instead of 6-4PP. In agreement with the previous report (Wakasugi et al., 2001), preincubation of the CPD substrate with UV-DDB resulted in a weak but detectable stimulation of dual incision in the XP-E cell extract, although quite large amounts of UV-DDB were required (Figure S6). In the presence of methylated ubiquitin, some stimulation by UV-DDB could still be observed.

To examine the direct involvement of ubiquitylation in

NER, we set up the reconstituted NER reaction with purified proteins. By using six purified essential NER factors (i.e., XPC-HR23B-centrin 2, XPA, XPF-ERCC1, XPG, transcription factor IIH [TFIIH], and replication protein A [RPA]), a significant level of dual incision could be detected with the internally radiolabeled 6-4PP substrate (Figure 6C, lane 2). The addition of the UV-DDB-E3 complex resulted in dose-dependent inhibition of the dual incision (lanes 3–5) if other ubiquitylating factors (E1, E2, and ubiquitin) were not present. Although the involvement of the ubiquitylating factors had little effect on the repair of 6-4PP (Figure 6D, lane 3), the inhibition caused by the UV-DDB-E3 complex appeared to be relieved at least partially in the presence of these factors (Figure 6D, compare lanes 4 and 5). The ubiquitylation of XPC under these reaction conditions was confirmed by immunoblotting (Figure 6E). In this reaction system, the efficiency of incision around CPD was too low to be detected. These results indicate that the elongation of polyubiquitin chains is important for NER of 6-4PP when UV-DDB is bound to the lesion.

Discussion

UV-DDB-Dependent Ubiquitylation of XPC
We have shown that the XPC protein is ubiquitylated in response to the UV irradiation of cells and that this ubiquitylation requires functional UV-DDB activity. It has been shown recently that UV-DDB associates in vivo with cullin 4A, Roc1, and COP9 signalosome, which suggests that this supercomplex may function as the E3 ligase complex (Groisman et al., 2003). The autoubiquitylation of cullin 4A subunit was indeed detected, but the physiological substrates of this E3 activity were not identified. Therefore, XPC is the first example of such an E3 substrate. This observation links the two known NER damage recognition factors and suggests a mechanism by which they operate together in NER.

Our present study demonstrates a direct physical interaction between XPC and UV-DDB that appears to be present even in unirradiated cells (Figure 3A). Moreover, in the absence of UV damage, the cullin 4A protein in the UV-DDB-E3 complex is not conjugated to Nedd8 (Groisman et al., 2003). This strongly suggests that the E3 may be inactivated through its association with the COP9 signalosome, which explains why XPC ubiquitylation is absent in unirradiated cells (Figure 7). However, when cells are irradiated with UV, UV-DDB-E3 translocates onto chromatin probably through its ability to interact with UV photolesions. Neddylated cullin 4A has been specifically detected in the chromatin bound fraction of UV-irradiated cells (Groisman et al., 2003). This suggests that the E3 associated with UV-DDB may be activated only when bound to UV-damaged chromatin. This also suggests that the ubiquitylation of XPC may occur exclusively on the damaged DNA (Figure 7). In our cell-free system, the addition of damaged DNA was not necessary for XPC ubiquitylation. This is not surprising, because we used the recombinant UV-DDB-E3 complex that lacks the COP9 signalosome and is thus constitutively active. For the two XP-E cell lines used in this study (XP2ROSV and XP82TO), mutations

in the *DDB2* gene leads to inactivation of UV-DDB (Nichols et al., 1996). This suggests that, in these cells, E3 may never be activated even after UV irradiation. In contrast, XPC is normally ubiquitylated in XP-A, -B, -D, -F, and -G cells (Figure 2A). These observations indicate that XPC ubiquitylation may depend solely on the presence of functional UV-DDB and not on subsequent steps in the NER pathway.

Although our UV-DDB-associated recombinant E3 complex was active in the absence of DNA (Figure 4), its activity seemed to be further stimulated by the presence of 6-4PP (Figure 5A). This strongly suggests that the binding of UV-DDB to the lesion may affect the activity of UV-DDB-associated E3. Unlike the effect of UV irradiation, XPC ubiquitylation was much less pronounced when cells were treated with chemicals such as 4-NQO (Figure S1). This may be related to the observation that UV-DDB poorly recognizes 4-NQO-induced lesions (Payne and Chu, 1994). We also found that the binding affinities of UV-DDB for bubble and loop structures are far lower than that for 6-4PP (Figure S4C). This suggests that UV-DDB is not a versatile damage recognition factor like XPC; rather, it specializes in recognizing UV lesions, particularly 6-4PP. Such biochemical properties of UV-DDB may explain why exposure to UV but not the chemical carcinogen 7,12-dimethylbenz-[a]anthracene induced skin tumors in *DDB2*-deficient mice (Itoh et al., 2004). Taken together, it appears that the activation of E3 and the consequent ubiquitylation of XPC are not associated with all GG-NER lesions; rather, the occurrence of these events depends on the binding affinity of UV-DDB for the induced lesions.

Roles of Ubiquitylation in GG-NER
Although XPC acquired polyubiquitin chains in our cell-free system, the UV-induced modification of XPC appeared to be reversible and did not induce degradation via the 26S proteasome. Mechanisms that protect the ubiquitylated XPC from degradation thus may exist. In regard to this, it has been noted that complex formation with HR23 proteins stabilizes XPC (Ng et al., 2003; Okuda et al., 2004), perhaps because this regulates its degradation via the ubiquitin/proteasome pathway. Notably, the UV-DDB-E3 complex also ubiquitylated two of its own subunits in vitro, namely DDB2 and cullin 4A. As reported previously (Fitch et al., 2003a; Rapic'-Otrin et al., 2002), DDB2 appeared to be degraded after UV irradiation (Figure S3). Thus, the fates of ubiquitylated XPC and DDB2 appear to be quite different, even though the two proteins are probably ubiquitylated by the same E3 molecules.

The DDB1/DDB2 heterodimer binds to 6-4PP with very high affinity and specificity (Fujiwara et al., 1999; Reardon et al., 1993; Treiber et al., 1992). Since the binding affinity of XPC for this lesion is much lower (Figure S4) and UV-DDB rapidly translocates into the locally irradiated area in the nucleus without functional XPC (Wakasugi et al., 2002), UV-DDB is probably the first NER factor to recognize and bind 6-4PP in vivo. Notably, although the addition of UV-DDB inhibited our NER reactions that were reconstituted with six purified essential proteins (Figure 6C), the reactions using the XP-E cell extract appeared to be much more resistant
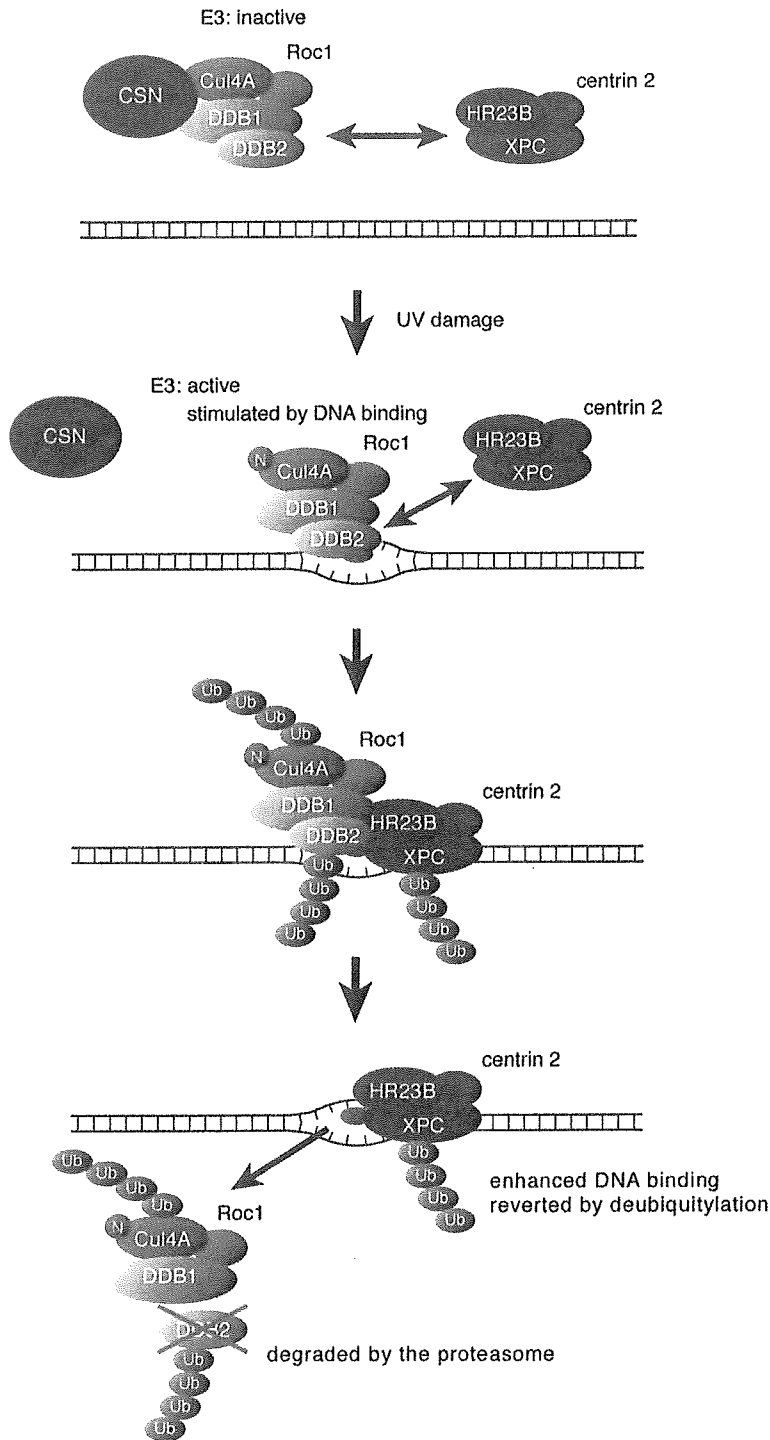
Figure 7. Model for UV-Induced UV-DDB-Dependent Ubiquitylation of XPC

In unirradiated cells, UV-DDB-associated E3 is inactivated by its interaction with the COP9 signalosome (CSN). Thus, XPC is not ubiquitylated, despite its interaction with UV-DDB. Upon UV irradiation, UV-DDB translocates onto the damaged chromatin by binding to lesions, particularly 6-4PP. Its dissociation from the CSN and the neddylation of cullin 4A (indicated by "N") activate E3. The binding of UV-DDB to the lesion further stimulates E3 activity. The activated UV-DDB-E3 then recruits XPC via protein-protein interaction, and XPC, DDB2, and cullin 4A are ubiquitylated at the lesion site. Polyubiquitylated UV-DDB loses its damaged DNA binding activity, whereas the DNA binding of XPC is potentiated by its ubiquitylation. This results in the displacement of UV-DDB by XPC on the lesion. The ubiquitylated DDB2 is degraded by the proteasome. The ubiquitylated form of XPC reverts to the unmodified form through deubiquitylation.

to UV-DDB (Figure 6A), which strongly suggests that specific factors are required for the repair of 6-4PP in the presence of UV-DDB. One can imagine that the extremely stable binding of UV-DDB to 6-4PP could prevent the subsequent binding of other GG-NER factors, including XPC. Based on our present results, we propose that UV-DDB-dependent polyubiquitylation is involved in the displacement of UV-DDB by XPC from

6-4PP (Figure 7). The evidence for this notion is as follows. First, UV-DDB appears to lose its high binding affinity for 6-4PP when DDB2 is extensively polyubiquitylated, whereas XPC polyubiquitylated under the same conditions displayed a higher DNA binding activity compared to its unmodified form (Figure 5). These alterations in DNA binding properties would certainly aid the replacement of UV-DDB by XPC. Second, the inhibition

of polyubiquitin chain elongation by adding K-less or methylated ubiquitin revealed the UV-DDB-dependent inhibition of 6-4PP repair in the XP-E cell extract (Figures 6A and 6B). Finally, the addition of the ubiquitylation factors to the reconstituted NER reaction removed the UV-DDB-dependent inhibition of 6-4PP repair (Figure 6D), although the incision activity was only partially restored under the conditions tested. This might be explained by the relatively unstable association of E3 in our preparation of the UV-DDB complex (Figure 5A), since UV-DDB that has lost E3 probably inhibits the repair of 6-4PP. Moreover, the reconstituted NER reaction may still be missing additional factors that are present in the crude cell extract and are specifically required when UV-DDB-dependent ubiquitylation occurs.

In XP-E cells lacking UV-DDB, GG-NER of 6-4PP is almost normal, even though UV-induced ubiquitylation of XPC is absent. The above model is consistent with this phenotype of XP-E cells, because it indicates that XPC ubiquitylation is only required when UV-DDB is present, since XPC is able to detect 6-4PP by itself without ubiquitylation. Notably, NER functions of UV-DDB have been documented mainly in connection with the repair of CPD rather than 6-4PP (Hwang et al., 1999; Tang et al., 2000). We have previously shown that the XPC complex by itself recognizes CPD very poorly, presumably because the distortion of the helix induced by the lesion is too small (Sugasawa et al., 2001). For such lesions, recognition by UV-DDB may facilitate the recruitment of other NER factors including XPC (Fitch et al., 2003b). From our in vitro experiments, the involvement of UV-DDB-dependent ubiquitylation in CPD repair was not clear, since stimulation of CPD repair by UV-DDB still appeared to occur in the absence of polyubiquitylation (Figure S6). However, the observed stimulation was nonetheless quite weak and required unphysiologically high concentrations of UV-DDB. This raises the possibility that even the in vitro NER reaction using the crude cell extract may require optimization before the precise roles of UV-DDB and ubiquitylation in CPD repair can be examined. However, since UV-DDB appears, upon extensive polyubiquitylation, to lose its binding activity to not only 6-4PP but also CPD (Figure 5A), it cannot be excluded that ubiquitylation may also be associated with CPD repair.

Given that XPC is able to recognize 6-4PP by itself, what is the biological significance of such a high binding affinity of UV-DDB for 6-4PP? Although many published studies indicate that the lack of UV-DDB barely affects the efficiency with which 6-4PP is repaired in vivo, it has been shown very recently that UV-DDB can facilitate the recruitment of XPC as well as other NER factors to sites containing 6-4PP, particularly when the number of induced 6-4PP lesions is relatively low (L.H.F. Mullenders, personal communication). We favor the idea that UV-DDB is involved in efficiently recruiting XPC to UV lesions, regardless of whether these lesions are CPD or 6-4PP, since this supports the biological relevance of our in vitro results that point to the roles ubiquitylation plays in the repair of 6-4PP. As proposed in Figure 7, one of the roles UV-induced XPC ubiquitylation may play is that it reinforces the DNA binding of XPC, which helps displace UV-DDB from the lesion (even though UV-DDB initially binds to the UV lesion

more strongly than XPC). These observations together appear to add quite novel insights into the damage recognition mechanisms involved in DNA repair, as well as to the functions of ubiquitylation. However, it cannot be excluded that the ubiquitylation of XPC and UV-DDB may play additional roles. For instance, polyubiquitylated XPC and/or DDB2 may be involved in signal transduction pathways that are activated in response to DNA damage. In addition, the degradation of DDB2 itself may serve as a certain intracellular signal. To fully understand the roles of UV-DDB-dependent ubiquitylation, it would be of great interest to generate mutant XPC and DDB2 molecules that specifically lack their interaction or ubiquitylation sites. In addition, it would be highly informative to identify the factors that interact specifically with ubiquitylated XPC and/or UV-DDB.

Experimental Procedures

Additional information can be found in the Supplemental Data.

Cell Lines and Cultures

WI38 VA13 cells as well as other human fibroblast cell lines derived from XP and CS patients were cultured at 37°C in Dulbecco's modified Eagle's medium containing 10% fetal bovine serum. Chinese hamster cells were cultured under the same conditions, except for the addition of L-proline with CHO-K1 cells. Stable V79 transformants expressing human DDB2 were established as described previously (Tang et al., 2000) and cultured in the presence of 500 μg/ml G418 (Invitrogen). A lymphoblastoid cell line (GM01646) from an XP-E patient was obtained from the Coriell Cell Repository and cultured in suspension with RPMI1640 medium containing 15% heat-inactivated fetal bovine serum. Mouse mammary carcinoma FM3A as well as its temperature-sensitive mutant ts85 cells were maintained at 33°C in suspension with RPMI1640 medium containing 10% calf serum.

Purified Protein Factors

Human XPC and His_6-tagged HR23B (HR23B-His) proteins were expressed and purified separately as described previously (Sugasawa et al., 2001). In vitro reconstitution of the XPC-HR23B-His heterodimer has also been described previously (Sugasawa et al., 2001). Centrin 2 was expressed in E. coli and purified as described (Araki et al., 2001).

Other NER factors except TFIIH were expressed in insect cells by using the baculovirus system. Detailed purification procedures are given in the Supplemental Data. The human TFIIH complex was purchased from ProteinOne. Rabbit E1 and human UbcH5a (E2) enzymes as well as ubiquitin (wild-type, K-less, or GST-tagged) were purchased from Boston Biochem, while wild-type ubiquitin was also obtained from Sigma.

In Vitro Ubiquitylation Assay

The standard reaction mixture (15 μl) contained 50 mM Tris-HCl (pH 7.6), 10 mM $MgCl_2$, 0.2 mM $CaCl_2$, 4 mM ATP, 1 mM dithiothreitol (DTT), bovine serum albumin (BSA; 1.5 μg), E1 (0.1 μg), E2 (0.4 μg), ubiquitin (5 μg), purified UV-DDB-E3 (20 ng), and XPC-HR23B-His. The reactions were incubated at 37°C for 1 hr, stopped by adding 1 μl of 0.5 M EDTA, and subjected to SDS-PAGE followed by immunoblot analyses using appropriate antibodies.

Damaged DNA Binding Assay

Details of DNA bead preparation are provided in the Supplemental Data. Binding reactions were performed at 30°C for 30 min in mixtures (15 μl) containing 50 mM Tris-HCl (pH 7.6), 5 mM $MgCl_2$, 0.2 mM $CaCl_2$, 2 mM ATP, 1 mM DTT, 0.1 M NaCl, BSA (1.5 μg), varied amounts of XPC-HR23B-His (together with a four times molar excess of centrin 2), and 12 μg of the paramagnetic beads containing 1 pmol of UV lesions or the corresponding amount of undamaged DNA as a control. Where indicated, UV-DDB-E3 (20 ng), E1 (0.1 μg), E2 (0.5 μg), and ubiquitin (wild-type or methylated; 10 μg) were

also included. After the reactions were stopped by adding 1 μl of 0.5 M EDTA, the supernatants were saved as "unbound" fractions. The beads were then washed twice with 50 μl of ice-cold wash buffer (50 mM Tris-HCl [pH 7.6], 5 mM $MgCl_2$, 0.2 mM $CaCl_2$, 0.1 M NaCl, 1 mM DTT) and suspended in SDS sample buffer. Aliquots of the unbound and bound fractions were subjected to SDS-PAGE followed by immunoblotting.

NER Dual Incision Assay

The internally ^{32}P-labeled, double-stranded circular DNA substrate that contains a single, site-specific 6-4PP or CPD, and whole-cell extract from the XP-E lymphoblastoid cells (GM01646) were prepared as described previously (Sugasawa et al., 2001). The standard reaction mixture (25 μl) contained 40 mM Hepes-KOH (pH 7.8), 5 mM $MgCl_2$, 2 mM ATP, 0.5 mM DTT, 70 mM NaCl, 5% glycerol, BSA (5.4 μg), the XP-E cell extract (100 μg of protein), 22.5 mM creatine phosphate (di-Tris; Sigma), creatine phosphokinase (0.5 μg; Sigma type I), and the ^{32}P-labeled DNA substrate (~1 × 10^5 cpm for 6-4PP and ~4 × 10^5 cpm for CPD, respectively). For the reconstituted NER, the reaction volume was reduced to 15 μl; the XP-E cell extract was replaced by FLAG-XPA (25 ng), RPA (100 ng), XPF-ERCC1-His (12 ng), XPG (12 ng), TFIIH (134 ng), XPC-HR23B-His (20 ng), and centrin 2 (5 ng); and the NaCl concentration was adjusted at 100 mM. Where indicated, E1 (0.1 μg), E2 (0.5 μg), ubiquitin (wild-type, K-less, or methylated), and varied amounts of UV-DDB or UV-DDB-E3 complex were also included. After incubation at 30°C for 1 hr, the DNA was purified and subjected to 10% denaturing PAGE followed by autoradiography.

Supplemental Data

Supplemental Data include six figures, Supplemental Experimental Procedures, and Supplemental References and can be found with this article online at http://www.cell.com/cgi/content/full/121/3/387/DC1/.

Acknowledgments

References

Aboussekhra, A., Biggerstaff, M., Shivji, M.K.K., Vilpo, J.A., Moncollin, V., Podust, V.N., Protic, M., Hübscher, U., Egly, J.-M., and Wood, R.D. (1995). Mammalian DNA nucleotide excision repair reconstituted with purified protein components. Cell 80, 859–868.

Araki, M., Masutani, C., Takemura, M., Uchida, A., Sugasawa, K., Kondoh, J., Ohkuma, Y., and Hanaoka, F. (2001). Centrosome protein centrin 2/caltractin 1 is part of the xeroderma pigmentosum group C complex that initiates global genome nucleotide excision repair. J. Biol. Chem. 276, 18665–18672.

Araújo, S.J., Tirode, F., Coin, F., Pospiech, H., Syväoja, J.E., Stucki, M., Hübscher, U., Egly, J.-M., and Wood, R.D. (2000). Nucleotide excision repair of DNA with recombinant human proteins: definition

of the minimal set of factors, active forms of TFIIH, and modulation by CAK. Genes Dev. 14, 349–359.

Batty, D., Rapic'-Otrin, V., Levine, A.S., and Wood, R.D. (2000). Stable binding of human XPC complex to irradiated DNA confers strong discrimination for damaged sites. J. Mol. Biol. 300, 275–290.

Bootsma, D., Kraemer, K.H., Cleaver, J.E., and Hoeijmakers, J.H.J. (1997). Nucleotide excision repair syndromes: xeroderma pigmentosum, Cockayne syndrome, and trichothiodystrophy. In The Metabolic Basis of Inherited Disease, C.R. Scriver, A.L. Beaudet, W.S. Sly, and D. Valle, eds. (New York: McGraw-Hill Book Co.), pp. 245–274.

Chu, G., and Chang, E. (1988). Xeroderma pigmentosum group E cells lack a nuclear factor that binds to damaged DNA. Science 242, 564–567.

Finley, D., Ciechanover, A., and Varshavsky, A. (1984). Thermolability of ubiquitin-activating enzyme from the mammalian cell cycle mutant ts85. Cell 37, 43–55.

Fitch, M.E., Cross, I.V., Turner, S.J., Adimoolam, S., Lin, C.X., Williams, K.G., and Ford, J.M. (2003a). The DDB2 nucleotide excision repair gene product p48 enhances global genomic repair in p53 deficient human fibroblasts. DNA Repair (Amst.) 2, 819–826.

Fitch, M.E., Nakajima, S., Yasui, A., and Ford, J.M. (2003b). In vivo recruitment of XPC to UV-induced cyclobutane pyrimidine dimers by the DDB2 gene product. J. Biol. Chem. 278, 46906–46910.

Friedberg, E.C. (2001). How nucleotide excision repair protects against cancer. Nat. Rev. Cancer 1, 22–33.

Fujiwara, Y., Masutani, C., Mizukoshi, T., Kondo, J., Hanaoka, F., and Iwai, S. (1999). Characterization of DNA recognition by the human UV-damaged DNA-binding protein. J. Biol. Chem. 274, 20027–20033.

Groisman, R., Polanowska, J., Kuraoka, I., Sawada, J., Saijo, M., Drapkin, R., Kisselev, A.F., Tanaka, K., and Nakatani, Y. (2003). The ubiquitin ligase activity in the DDB2 and CSA complexes is differentially regulated by the COP9 signalosome in response to DNA damage. Cell 113, 357–367.

Hoeijmakers, J.H.J. (2001). Genome maintenance mechanisms for preventing cancer. Nature 411, 366–374.

Hwang, B.J., Toering, S., Francke, U., and Chu, G. (1998). p48 activates a UV-damaged DNA-binding factor and is defective in xeroderma pigmentosum group E cells that lack binding activity. Mol. Cell. Biol. 18, 4391–4399.

Hwang, B.J., Ford, J.M., Hanawalt, P.C., and Chu, G. (1999). Expression of the p48 xeroderma pigmentosum gene is p53 dependent and is involved in global genome repair. Proc. Natl. Acad. Sci. USA 96, 424–428.

Itoh, T., Linn, S., Ono, T., and Yamaizumi, M. (2000). Reinvestigation of the classification of five cell strains of xeroderma pigmentosum group E with reclassification of three of them. J. Invest. Dermatol. 114, 1022–1029.

Itoh, T., Cado, D., Kamide, R., and Linn, S. (2004). DDB2 gene disruption leads to skin tumors and resistance to apoptosis after exposure to ultraviolet light but not a chemical carcinogen. Proc. Natl. Acad. Sci. USA 101, 2052–2057.

Masutani, C., Sugasawa, K., Yanagisawa, J., Sonoyama, T., Ui, M., Enomoto, T., Takio, K., Tanaka, K., van der Spek, P.J., Bootsma, D., et al. (1994). Purification and cloning of a nucleotide excision repair complex involving the xeroderma pigmentosum group C protein and a human homolog of yeast RAD23. EMBO J. 13, 1831–1843.

Matsumoto, Y., Yasuda, H., Marunouchi, T., and Yamada, M. (1983). Decrease in uH2A (protein A24) of a mouse temperature-sensitive mutant. FEBS Lett. 151, 139–142.

Mu, D., Park, C.H., Matsunaga, T., Hsu, D.S., Reardon, J.T., and Sancar, A. (1995). Reconstitution of human DNA repair excision nuclease in a highly defined system. J. Biol. Chem. 270, 2415–2418.

Ng, J.M.Y., Vermeulen, W., van der Horst, G.T.J., Bergink, S., Sugasawa, K., Vrieling, H., and Hoeijmakers, J.H.J. (2003). A novel regulation mechanism of DNA repair by damage-induced and RAD23-dependent stabilization of xeroderma pigmentosum group C protein. Genes Dev. 17, 1630–1645.

Nichols, A.F., Ong, P., and Linn, S. (1996). Mutations specific to the xeroderma pigmentosum group E Ddb– phenotype. J. Biol. Chem. *271*, 24317–24320.

Okuda, Y., Nishi, R., Ng, J.M.Y., Vermeulen, W., van der Horst, G.T.J., Mori, T., Hoeijmakers, J.H.J., Hanaoka, F., and Sugasawa, K. (2004). Relative levels of the two mammalian Rad23 homologs determine composition and stability of the xeroderma pigmentosum group C protein complex. DNA Repair (Amst.) *3*, 1285–1295.

Otrin, V.R., McLenigan, M., Takao, M., Levine, A.S., and Protic, M. (1997). Translocation of a UV-damaged DNA binding protein into a tight association with chromatin after treatment of mammalian cells with UV light. J. Cell Sci. *110*, 1159–1168.

Payne, A., and Chu, G. (1994). Xeroderma pigmentosum group E binding factor recognizes a broad spectrum of DNA damage. Mutat. Res. *310*, 89–102.

Rapic'-Otrin, V., McLenigan, M.P., Bisi, D.C., Gonzalez, M., and Levine, A.S. (2002). Sequential binding of UV DNA damage binding factor and degradation of the p48 subunit as early events after UV irradiation. Nucleic Acids Res. *30*, 2588–2598.

Rapic'-Otrin, V., Navazza, V., Nardo, T., Botta, E., McLenigan, M., Bisi, D.C., Levine, A.S., and Stefanini, M. (2003). True XP group E patients have a defective UV-damaged DNA binding protein complex and mutations in DDB2 which reveal the functional domains of its p48 product. Hum. Mol. Genet. *12*, 1507–1522.

Reardon, J.T., Nichols, A.F., Keeney, S., Smith, C.A., Taylor, J.S., Linn, S., and Sancar, A. (1993). Comparative analysis of binding of human damaged DNA-binding protein (XPE) and *Escherichia coli* damage recognition protein (UvrA) to the major ultraviolet photoproducts: T[c,s]T, T[t,s]T, T[6-4]T, and T[Dewar]T. J. Biol. Chem. *268*, 21301–21308.

Riedl, T., Hanaoka, F., and Egly, J.-M. (2003). The comings and goings of nucleotide excision repair factors on damaged DNA. EMBO J. *22*, 5293–5303.

Shivji, M.K.K., Eker, A.P.M., and Wood, R.D. (1994). DNA repair defect in xeroderma pigmentosum group C and complementing factor from HeLa cells. J. Biol. Chem. *269*, 22749–22757.

Sugasawa, K., Ng, J.M.Y., Masutani, C., Iwai, S., van der Spek, P.J., Eker, A.P.M., Hanaoka, F., Bootsma, D., and Hoeijmakers, J.H.J. (1998). Xeroderma pigmentosum group C protein complex is the initiator of global genome nucleotide excision repair. Mol. Cell *2*, 223–232.

Sugasawa, K., Okamoto, T., Shimizu, Y., Masutani, C., Iwai, S., and Hanaoka, F. (2001). A multistep damage recognition mechanism for global genomic nucleotide excision repair. Genes Dev. *15*, 507–521.

Sugasawa, K., Shimizu, Y., Iwai, S., and Hanaoka, F. (2002). A molecular mechanism for DNA damage recognition by the xeroderma pigmentosum group C protein complex. DNA Repair (Amst.) *1*, 95–107.

Tang, J.Y., Hwang, B.J., Ford, J.M., Hanawalt, P.C., and Chu, G. (2000). Xeroderma pigmentosum p48 gene enhances global genomic repair and suppresses UV-induced mutagenesis. Mol. Cell *5*, 737–744.

Tornaletti, S., and Hanawalt, P.C. (1999). Effect of DNA lesions on transcription elongation. Biochimie *81*, 139–146.

Treiber, D.K., Chen, Z., and Essigmann, J.M. (1992). An ultraviolet light-damaged DNA recognition protein absent in xeroderma pigmentosum group E cells binds selectively to pyrimidine (6-4) pyrimidone photoproducts. Nucleic Acids Res. *20*, 5805–5810.

Volker, M., Moné, M.J., Karmakar, P., van Hoffen, A., Schul, W., Vermeulen, W., Hoeijmakers, J.H.J., van Driel, R., van Zeeland, A.A., and Mullenders, L.H.F. (2001). Sequential assembly of the nucleotide excision repair factors in vivo. Mol. Cell *8*, 213–224.

Wakasugi, M., Shimizu, M., Morioka, H., Linn, S., Nikaido, O., and Matsunaga, T. (2001). Damaged DNA-binding protein DDB stimulates the excision of cyclobutane pyrimidine dimers in vitro in concert with XPA and replication protein A. J. Biol. Chem. *276*, 15434–15440.

Wakasugi, M., Kawashima, A., Morioka, H., Linn, S., Sancar, A., Mori, T., Nikaido, O., and Matsunaga, T. (2002). DDB accumulates at DNA damage sites immediately after UV irradiation and directly stimulates nucleotide excision repair. J. Biol. Chem. *277*, 1637–1640.